Journal of Oceanography (2020) 76:71–89
https://doi.org/10.1007/s10872-019-00534-5

REVIEW

Non-traditional stable isotope geochemistry of marine ferromanganese crusts and nodules

Yazhou Fu[1]

Received: 29 January 2019 / Revised: 31 October 2019 / Accepted: 3 November 2019 / Published online: 9 November 2019

Abstract

Marine ferromanganese crusts and nodules, which contain a variety of metals, are potential seabed mineral resources. Given their low growth rates, they are regarded as condensed stratigraphic sections that archive millions of years of paleoceanographic information. Ferromanganese crusts and nodules incorporate trace elements like Cu, Zn, Mo, Tl and Ni during growth. The non-traditional isotopic systems of these metals are increasingly being developed as powerful tracers in the modern ocean and as proxies for the paleo-ocean, due to their tendency to be fractionated by redox-related and/or biological processes. In recent years, both the global variations of metal stable isotopes in ferromanganese crust/nodule surface scrapings and some depth profiles through the ferromanganese crusts were systematically analysed. These studies established the isotopic variability present in ferromanganese crusts, nodules and seawater, explored the isotopic fractionation mechanisms associated with the formation of ferromanganese deposits, and determined whether these ferromanganese crusts can be used as documents of deep water metal isotope compositions and long-term seawater isotope variations. In addition, some isotopes of ferromanganese deposits have been successfully applied to constrain the metal sources and geochemical cycles in the ocean, reconstruct paleo-oceanic redox conditions and seawater isotope record, and reveal continental weathering and climate changes. Nevertheless, it is worth noting that a few limitations of current applications of some non-traditional isotopes as paleoceanographic proxies still remain. Therefore, there is still a great need for a community effort to develop and enhance non-traditional isotope geochemistry of marine ferromanganese crusts and nodules.

Keywords Marine ferromanganese crusts and nodules · Seawater · Isotope composition · Isotopic fractionation · Non-traditional stable isotopes

Abbreviations

REE	Rare earth element
TIMS	Thermal ionization mass spectrometry
MC-ICP-MS	Multiple collector inductively coupled plasma mass spectrometry
XANES	X-Ray absorption near edge structure
EXAFS	Extended X-ray absorption fine structure

1 Introduction

Marine ferromanganese (Fe–Mn) crusts and nodules have gained recognition as potential future mineral resources for a wide variety of elements such as Co, Ti, Mn, Ni, Pt, Te, Mo, REEs etc. for crusts and Ni, Cu, Co, Mn, Mo, Li and REEs for nodules (Hein et al. 2000, 2013). Having formed deep in the oceans and grown slowly (1–10 mm/Myr), Fe–Mn crusts and nodules have experienced geological histories of millions or even tens of millions of years (Burton et al. 1999; Frank 2002; Fu et al. 2005; Klemm et al. 2005; Ling et al. 2005; Usui et al. 2017). They are formed by long-term interactions between the oceanic lithosphere and other Earth spheres that include the hydrosphere, the Earth's crust and mantle, and long-term couplings among a variety of metallogenic factors (Christensen et al. 1997; Banakar and Hein 2000; Hein 2004; Hein and Koschinsky 2014; Conrad et al. 2017). Their formations not only record their mineralization sources and formation mechanisms, but they also record the

✉ Yazhou Fu
fuyazhou@mail.gyig.ac.cn

[1] State Key Laboratory of Ore Deposit Geochemistry, Institute of Geochemistry, Chinese Academy of Sciences, Guiyang, China

history of oceanic and climatic conditions (Ling et al. 1997; Zhu et al. 2000; Banakar and Hein 2000; Hein 2004; Nielsen et al. 2009; Hein and Koschinsky 2014; Gueguen et al. 2016; Usui et al. 2017).

Radiogenic isotopes (e.g., Pb, Sr, Nd, Os, Hf) in Fe–Mn crusts and nodules have been extensively investigated to resolve fundamental paleoceanographic issues such as the evolution of oceanic circulation, changes in the marine source and/or sink fluxes, modifications in continental weathering, impacts of hydrothermal inputs and age determinations of marine Fe–Mn deposits (McMurtry et al. 1994; Peucker-Ehrenbrink et al. 1995; Christensen et al. 1997; Burton et al. 1999; Lee et al. 1999; Ling et al. 1997, 2005; O'Nions et al. 1998; Frank 2002; Frank et al. 1999; Fu et al. 2005; Klemm et al. 2005; Chen et al. 2013). In recent years, with the rapid developments in multiple collector inductively coupled plasma mass spectrometry (MC-ICP-MS) and thermal ionization mass spectrometry (TIMS), isotopes of more elements such as Fe, Cu, Zn, Mo, Cd, Mg and Tl can be accurately measured (Table 1). When compared to traditional stable isotopes (H, C, N, O and S), these "non-traditional" stable isotopes have some unique geochemical characteristics. Their concentrations vary greatly in different geological reservoirs, many of them are redox-sensitive and/or biologically active elements, and, their bonding environments differ from those of traditional stable isotopes (Hoefs 2015; Teng et al. 2017). These characteristics make the different elements susceptible to different fractionation mechanisms, and by extension, make them powerful proxies in a variety of research realms including cosmochemistry, environmental geochemistry, marine geochemistry, petrology, and mineral deposits studies (Jiang et al. 2000; Zhu et al. 2000; Siebert et al. 2003; Rehkämper et al. 2004; Young and Galy 2004; Albarède 2004; Horner et al. 2010; Huh et al. 2001; Little et al. 2014a; Gueguen et al. 2016; Teng et al. 2017).

In the marine environment, authigenic Fe–Mn oxides precipitate from seawater, incorporating many dissolved trace elements such as Cu, Zn, Mo, Tl and Ni, whose isotopic compositions are new proxies for additional evidence regarding the causes and effects of changes in ocean chemistry and climate (Chu et al. 2006; Nielsen et al. 2009; Gall et al. 2013; Goto et al. 2015). Fe–Mn crusts and nodules are ideal choice to study non-traditional isotopic geochemistry for these reasons: (1) their elevated concentrations of various metal elements can meet the required amounts for samples with accurate isotope measurements of multiple elements simultaneously (Hein and Koschinsky 2014; Little et al. 2014a); (2) large isotope fractionation was usually produced during oceanic low-temperature geochemical processes in which Fe–Mn deposits were formed (Maréchal et al. 2000; Barling et al. 2001; Rehkämper et al. 2004; Chan and Hein 2007; Gall et al. 2013); (3) they represent a useful analogue for the sorptive output to dispersed Fe–Mn oxide phases present throughout marine sediments deposited under oxic conditions (Barling and Anbar 2004; Gall et al. 2013; Little et al. 2014a); (4) they control the concentration of some elements and the redox state of some metals in the global ocean (e.g., Fe, Cu, and Mo) (Barling et al. 2001; Anbar and Rouxel 2007; Little et al. 2014a; Hein and Koschinsky 2014); (5) they have proven potential as documents of past chemical and isotopic compositions of various elements dissolved in ocean deep waters (Burton et al. 1999; Frank 2002; Ling et al. 2005; Hein and Koschinsky 2014; Usui et al. 2017).

Up to very recently, pioneering studies were done on the non-traditional isotopic geochemistry of Fe–Mn crusts and nodules. Their works have not only primarily determined the isotope compositions and evolving characteristics of Fe–Mn crusts and nodules but have also revealed the isotope fractionations between seawater and Fe–Mn deposits, and associated isotopic fractionation mechanisms (Zhu et al. 2000; Maréchal et al. 2000; Rehkämper et al. 2002; Levasseur et al. 2004; Albarède 2004; Barling and Anbar 2004; Chan and Hein 2007; Schmitt et al. 2009; Gall et al. 2013). In addition, some studies discussed potential applications of these archives as constraining marine metal geochemical cycle and ocean isotope budget, reconstructing paleo-oceanic redox conditions, seawater isotope record and past changes in Earth's marine and climatic conditions (Zhu et al. 2000; Maréchal et al. 2000; Siebert et al. 2003; Rehkämper et al. 2004; Chan and Hein 2007; Horner et al. 2010; Rose-Koga and Albarede 2010; Little et al. 2014a; Gueguen et al. 2016). This paper summarizes the recent advance, important application and future direction of non-traditional isotope studies in marine Fe–Mn nodules and crusts.

2 Sample preparation and isotopic analyses

The development of the geochemistry of non-traditional stable isotopes fell behind that of light stable isotope (H, O, C and S) and radiogenic isotopes (Nd, Sr, Pb and Os) primarily for analytical techniques. In recent years, the analytical issues were solved with the development of MC-ICP-MS, which made it possible to measure these new isotopes rapidly and precisely that is sufficient for the resolution of small isotopic variations. MC-ICP-MS is becoming the instrument of choice for non-traditional stable isotope analysis because of the high ionization efficiency of the high-temperature Ar plasma and rapid sample throughput (Albarède and Beard 2004). Moreover, because instrumental mass bias varies relatively stable during the course of an analytical session, corrections for instrumental mass bias can be made by bracketing standards and by comparison to the mass bias inferred from an element of similar mass added to the

Table 1 Summary of non-traditional stable isotopes abundance, standards and concentration in seawater, Fe–Mn crusts and nodules

Element	Isotopes abundance	Delta notation	Standard reference material	Residence time in the ocean	Elemental concentration of modern seawater	Elemental concentration of Fe–Mn crust[a]	Elemental concentration of Fe–Mn nodules[b]
Fe	^{54}Fe (5.84%), ^{56}Fe (91.76%), ^{57}Fe (2.12%), ^{58}Fe (0.28%)	δ^{56}Fe ($\delta^{56/54}$Fe)	IRMM-014	70–200 years (Johnson et al. 1997)	< 1 nmol kg^{-1} (Johnson et al. 1997)	16.9%	5.92%
Cu	^{63}Cu (69.17%), ^{65}Cu (30.83%)	δ^{65}Cu ($\delta^{65/63}$Cu)	NIST SRM 976	5400 years (Little et al. 2014a)	0.5–6 nmol kg^{-1} (Coale and Bruland 1988)	976 ppm	10,631 ppm
Zn	^{64}Zn (48.63%), ^{66}Zn (27.90%), ^{67}Zn (4.10%), ^{68}Zn (18.75%), ^{70}Zn (0.62%)	δ^{66}Zn ($\delta^{68/64}$Zn)	JMC 3-0749 L, JMC-Lyon	11,000 years (Little et al. 2014a)	0.1–10 nmol kg^{-1} (Bermin et al. 2006)	668 ppm	1385 ppm
Mo	^{92}Mo (14.84%), ^{94}Mo (9.25%), ^{95}Mo (15.92%), ^{96}Mo (16.68%), ^{97}Mo (9.55%), ^{98}Mo (24.13%), ^{100}Mo (9.63%)	δ^{98}Mo ($\delta^{98/95}$Mo)	NIST SRM 3134, JMC Mo, MOMO, Alfa Aesar Mo	800,000 years (Firdaus et al. 2008), 400,000 years (Miller et al. 2011)	107 nmol kg^{-1} (Collier 1985)	461 ppm	587 ppm
Tl	^{203}Tl (29.5%), ^{205}Tl (70.5%)	ε^{205}Tl ($\varepsilon^{205/203}$Tl)	NIST SRM 997	18,500 years (Flegal and Patterson 1985; Rehkämper and Nielsen 2004)	64 pmol kg^{-1} (Flegal and Patterson 1985)	155 ppm	129 ppm
Cd	^{106}Cd (1.25%), ^{108}Cd (0.89%), ^{110}Cd (12.49%), ^{111}Cd (12.80%), ^{112}Cd (24.13%), ^{113}Cd (12.22%), ^{114}Cd (28.73%), ^{116}Cd (7.49%)	ε^{114}Cd ($\varepsilon^{114/110}$Cd)	Alfa Cd Zürich, JMC Cd Mainz, NIST SRM 3108	50,000 years (Bewers and Yeats 1977)	< 0.03 nmol kg^{-1} (< 150 m), 0.3–0.9 nmol kg^{-1} (> 900 m) (Ripperger et al. 2007)	3.59 ppm	18.8 ppm
Li	^{6}Li (7.5%), ^{7}Li (92.5%)	δ^{7}Li ($\delta^{7/6}$Li)	NIST SRM 8545	1.2 Ma (Huh et al. 1998)	26 µmol kg^{-1} (Riley and Tongudai 1964)	2.92 ppm	129 ppm
Mg	^{24}Mg (78.99%), ^{25}Mg (10.00%), ^{26}Mg (11.01%)	δ^{26}Mg ($\delta^{26/24}$Mg)	DSM-3	13 Ma (Berner and Berner 1987)	53 mmol kg^{-1} (Young and Galy 2004)	1.1%	1.88%
Ni	^{58}Ni (68.08%), ^{60}Ni (26.22%), ^{61}Ni (1.14%), ^{62}Ni (3.63%), ^{64}Ni (0.93%)	δ^{60}Ni ($\delta^{60/58}$Ni)	SRM 986 (NIST)	10,000 years (Sclater et al. 1976), 30,000 years (Cameron and Vance 2014), 4000 years (Li and Schoonmaker 2003)	2–12 nmol kg^{-1} (MBARI 2012)	4209 ppm	13,159 ppm

[a]Data are mean of N. Pacific Prime Zone from Hein and Koschinsky (2014)

[b]Data are mean of CCZ nodules from Hein and Koschinsky (2014), Tl data from Peru Basin nodules

analyte (Halliday et al. 1995; Rehkämper and Halliday 1999; Galy et al. 2001; Bermin et al. 2006; Wieser et al. 2007; Millet et al. 2012). Although stable isotope analyses by MC-ICP-MS still present a series of challenges, this method has come to dominate non-traditional stable isotopes research as such challenges have been addressed one by one.

Prior to chemical purification, the powdered samples must be leached and digested to dispose of any detrital material and achieve complete dissolution, because the mineral composition in marine Fe–Mn deposits is complex and the contents of various metal elements are high. In most studies, samples were leached in 6 M hydrochloric acid and any undissolved (detrital) material was eliminated from the solution by centrifugation (Maréchal et al. 1999; Zhu et al. 2000; Rehkämper et al. 2002; Horner et al. 2010; Gall et al. 2013). In addition, sequential step-leaching experiments were performed for optimal extraction of Li and Mg associated with the respective Fe–Mn oxide phases, because the occurrence states of these two elements in Fe–Mn nodules and crusts are different from those of other elements such as Cu, Zn, Mo and Ni (Chan and Hein 2007; Fu and Wang 2012). For Li isotope, samples were subjected to a two-step leaching using acetic acid and hydrochloric acid to leach out loosely bound Li and more tightly bound Li in the Fe–Mn oxides–oxyhydroxides (Chan and Hein 2007). For Mg isotope, samples were subjected to a series of incremental leaching steps, various concentrations of ammonium acetate, acetic acid, hydroxylamine hydrochloride, to extract Mg from different phases not associated with detrital material (including surface adsorbed Mg, and those associated with carbonates, Fe–Mn oxides) (Fu and Wang 2012). The precision of non-traditional stable isotopic measurements depends on the quality of the chemical extraction and on the correction of the instrumental bias. The high purity of the final target metal fraction is needed to remove both isobaric interferences and matrix interferences. As target isotopes can be fractionated during ion-exchange chromatography, the chemical procedure requires quantitative yields, unless a double-spike is added pre-column chemistry. The chemical purification of target metal is generally made by a combination of anion or/and cation exchange chromatography, making use of different affinities of the metals for the ion exchange resins in different strengths of acid media (Barling et al. 2001; Maréchal and Albarède 2002; Nielsen et al. 2004; Dauphas et al. 2009; Millet et al. 2012). In addition, some elements present in Fe–Mn nodules and crusts can hardly separate effectively, thus, a number of new element-specific resins are continually being developed as the need for new applications is encountered. References providing detailed descriptions of purification techniques for the metals discussed here include: Fe, Zhu et al. (2000); Cu and Zn, Maréchal et al. (1999); Mo, Barling et al. (2001); Cd, Schmitt et al. (2009); Tl, Rehkämper and Halliday (1999); Li, Chan and Hein (2007); Mg, Teng et al. (2007); Ni, Cameron et al. (2009).

3 Non-traditional stable isotopes in the ocean and marine Fe–Mn deposits

3.1 Iron (Fe) isotopes

As the metal element with the highest abundance in the solar system, iron, one of the most important elements of variable valency, is the essential nutrition element for life. Fe has four naturally occurring stable isotopes (Table 1): ^{54}Fe (5.84%), ^{56}Fe (91.76%), ^{57}Fe (2.12%) and ^{58}Fe (0.28%). Natural mass-dependent Fe isotope variations span a range of up to 5‰ in ^{56}Fe/^{54}Fe ratios, commonly expressed as δ^{56}Fe or ε^{57}Fe relative to the international standard IRMM-14. Previous studies have shown that the conversion formula between δ^{56}Fe and δ^{57}Fe is $\delta^{56}\text{Fe} = 0.677 \times \delta^{57}\text{Fe}$ (Zhu et al. 2001; Beard and Johnson 2004).

In the modern ocean, Fe demonstrates low concentrations (< 1 nmol/L) and short residence times (70–200 years) (Johnson et al. 1997). Dissolved Fe in seawater is primarily Fe^{3+} and Fe^{2+}, both of which exist in the form of free ions or inorganic and organic complexes. The sources for oceanic Fe include atmospheric dust, river runoff, hydrothermal vents, reducing sediments along continental margins, and oxic seafloor sediments, in which atmospheric dust is the main source (Beard et al. 2003; Anbar and Rouxel 2007; Conway and John 2014). Fe–Mn nodules and crusts, clastic sediments, and carbonates are the sinks for Fe in seawater (Anbar and Rouxel 2007; Conway and John 2014). Fe concentration is not uniformly distributed in the oceans. To take the seawater profile of the Pacific Ocean SAFe station as an example, Fe concentration in the shallow water (< 100 m) is low (< 0.1 nmol/kg), the concentration in the intermediate water (1000–1500 m) is highest (0.7 nmol/kg), and the concentration in the deep water (below 2000 m) is low (0.4–0.5 nmol/kg) again (Conway and John 2015). Similarly, Fe isotope compositions are not uniformly distributed in the oceans. The range of δ^{56}Fe in the seawater of Atlantic Ocean is −0.64‰ to +0.80‰ (Conway and John 2014; Fitzsimmons et al. 2015), whereas that in the Pacific Ocean is −0.64‰ to + 0.58‰ (Radic et al. 2011; Conway and John 2015). The δ^{56}Fe of the seawater profile at the SAFe station ranges from −0.6‰ to +0.1‰ (Conway and John 2015). These studies indicate that oceanic Fe isotope compositions demonstrate significant fractionation between different ocean basins and between shallow, intermediate, and deep seawater.

It is well-known that Fe is actively involved in key biogeochemical processes and has a variety of potential sources to the oceans, therefore, the record of Fe isotopes in Fe–Mn

deposits has attracted significant interest (Zhu et al. 2000; Beard et al. 2003; Levasseur et al. 2004; Chu et al. 2006; Horner et al. 2015; Marcus et al. 2015).

The δ^{57}Fe of the surface scrapings of hydrogenetic Fe–Mn crusts from global oceans ranges between −1.2 and −0.1‰ (converted to δ^{56}Fe is between −0.81 and −0.07‰) (Fig. 1), and the isotope changes are irrelevant to the growth rates of the crusts, and there is no significant basin to basin trends or relationships with expected hydrothermal contributions (Levasseur et al. 2004). δ^{56}Fe variations in Fe–Mn deposits are mainly controlled by the relative proportions of Fe from aerosols (~0‰) and Fe from mid-oceanic-ridge hydrothermal fluids (−0.5‰ to −1‰), there is no Fe isotopic fractionation between seawater Fe and the Fe–Mn oxyhydroxides during crust growth, which is unlikely considering the variety of Fe isotope fractionation processes in hydrothermal plumes (Beard et al. 2003).

Some studies have established Fe isotope depth profiles for several marine Fe–Mn crusts and nodules, and identified different variations in Fe isotope compositions (Fig. 2)

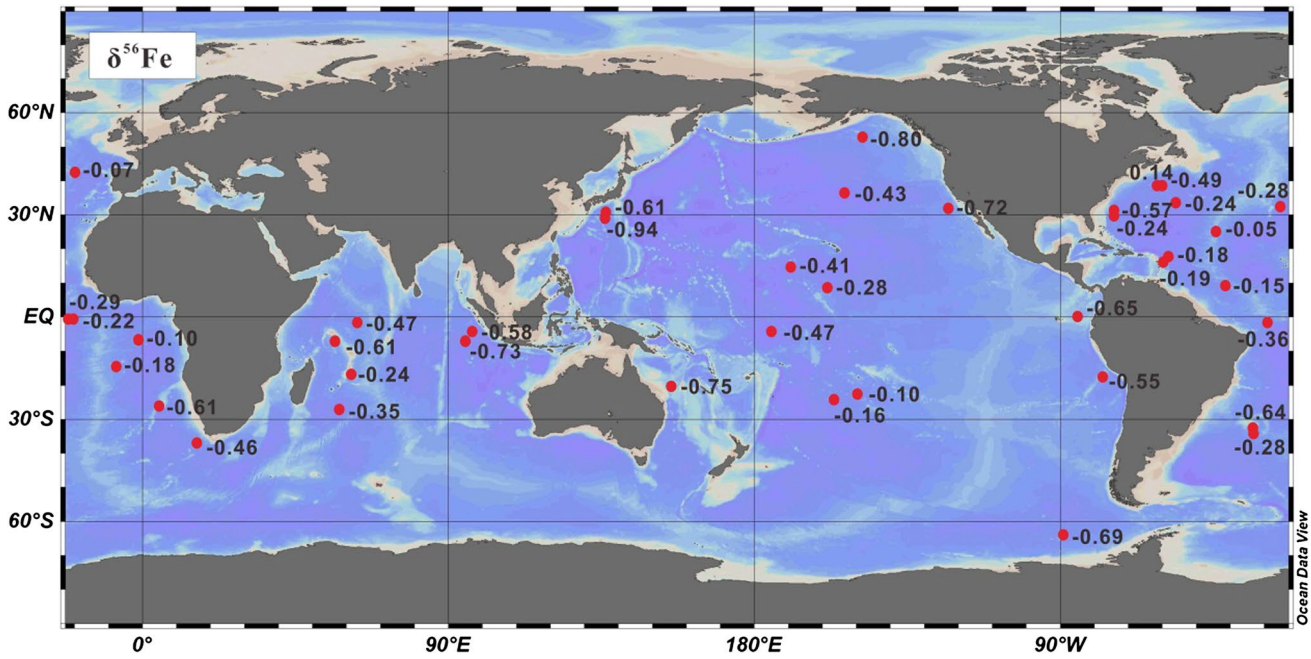

Fig. 1 Map of marine Fe–Mn nodules and crusts locations and the δ^{56}Fe values of surface scrapings from each sample. Data from Zhu et al. (2000), Levasseur et al. (2004), Chu et al. (2006), Marcus et al. (2015), Horner et al. (2015)

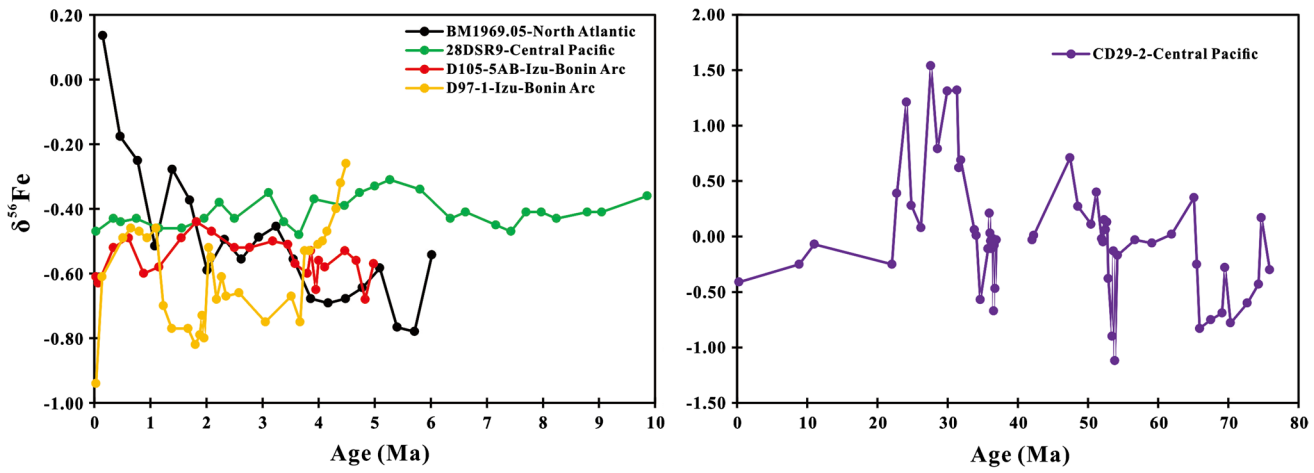

Fig. 2 Temporal δ^{56}Fe record from selected marine Fe–Mn crusts. The BM1969.05 crust profile is from Zhu et al. (2000), the 28DSR9, D105-5AB and D97-1 crust profiles are from Chu et al. (2006), the CD29-2 crust profile is from Horner et al. (2015)

(Zhu et al. 2000; Chu et al. 2006; Horner et al. 2015; Marcus et al. 2015). The Northwest Atlantic Fe–Mn crust BM1969.05 has a significant ε^{57}Fe changes, with ε^{57}Fe ranging between −11.5 and +2.0 (converted to δ^{56}Fe is between −0.78 and 0.14‰) since 6 Ma (Fig. 2), and the Fe isotope variations predominantly reflect those of iron input from terrigenous sources and provide no evidence for biologically induced mass fractionation within the North Atlantic Deep Water (Zhu et al. 2000). The Central Pacific crust 28DSR9 has a relatively stable Fe isotope composition (δ^{56}Fe = −0.41‰ ± 0.05‰) since 10 Ma (Fig. 2), the Izu-Bonin back arc crust D105-5AB also has a relatively stable Fe isotope composition (−0.55‰ ± 0.06‰) since 5 Ma (Fig. 2), it indicates that despite the significant changes in the inputs of Fe into the ocean surface via atmospheric particles since 10 Ma, the input pathway for Fe into the deep ocean has remained stable (Chu et al. 2006). However, the Izu-Bonin back arc crust D97-1 demonstrates a large range of δ^{56}Fe (Fig. 2), it is negatively correlated to the concentrations of Mn, Mg, Ni, Cu, Zn, Mo and V, and the decreases in δ^{56}Fe with respect to time are consistent with the periods of intense hydrothermal input. However, crust D105-5AB, which is only 100 km from D97-1, did not record the increase in Fe input via the hydrothermal, which indicates that the hydrothermal isolated pathways for Fe input may have migrated in the back arc (Chu et al. 2006). The central Pacific Fe–Mn crust CD29-2 has a range of δ^{56}Fe values from −1.12‰ to +1.54‰ along 76 Ma (Horner et al. 2015) (Fig. 2), this range encompasses the data of δ^{56}Fe measured for dissolved and particulate Fe from open ocean seawater and oxygen minimum zones (Conway and John 2014; Chever et al. 2015). Horner et al. (2015) proposed that heavy δ^{56}Fe values of seawater (up to 2.2‰) may result from the modification of deeply sourced Fe by precipitation of isotopically light Fe sulphides, by considering a fractionation factor during crust uptake of $\Delta^{56}Fe_{FeMn-SW} = -0.77 \pm 0.06$‰. The South Pacific Fe–Mn nodule has the δ^{56}Fe values from −0.16‰ to −0.07‰ over a period of 4 Ma, it suggests that constant Fe isotope values is irrelevant to the diversity of Fe mineral phases identified in the nodule layers (e.g., feroxyhite, goethite, lepidocrocite, and poorly ordered ferrihydrite-like phases). Hence, the results indicate that mineral alteration did not affect the primary Fe isotopic composition of the nodule (Marcus et al. 2015).

3.2 Copper (Cu) isotopes

Cu is a siderophile and highly chalcophile element (Siebert et al. 2011), mainly exists as sulfides or sulfate minerals in nature. Cu has three chemical valences, 0, +1 and +2, which enables Cu to have various geochemical behaviours under different redox conditions so that Cu can exist in a variety of minerals, rocks, fluids, and organisms and participate in all types of geochemical processes and life activities (Albarède 2004). Cu has two naturally occurring stable isotopes (Table 1): ^{63}Cu (69.17%) and ^{65}Cu (30.83%) (Shields et al. 1964). Natural mass-dependent variations in ^{65}Cu/^{63}Cu span 10‰ (Mathur et al. 2005). Cu isotopes are usually expressed relative to NIST SRM 976 as δ^{65}Cu. With the continuous decrease of international standard NIST SRM 976, the new alternative ideal standard material has yet to be unified.

Cu plays an important role as a micronutrient for organisms in the ocean. Dissolved Cu has concentrations of 0.5–6 nmol kg^{-1} in seawater and mostly complexes with organic ligands, which results in very low concentrations (fmol kg^{-1} to pmol kg^{-1}) of the free Cu^{2+} ion (Coale and Bruland 1990; Thompson et al. 2014). Vertical distributions of dissolved Cu are of the nutrient-scavenging hybrid type (Bruland and Lohan 2003). The residence time of Cu in ocean is 5400 years (Little et al. 2014a). Sources for oceanic Cu include rivers, hydrothermal inputs, and atmospheric depositions, whereas the main sinks for Cu are ferromanganese oxides and carbonate depositions (Little et al. 2014a). Seawater from the Indian and the Pacific Oceans and different depths of the Northeastern Pacific has significant differences in Cu isotope compositions (Bermin et al. 2006; Vance et al. 2008; Takano et al. 2014). δ^{65}Cu values of seawater from the Indian and the Pacific range between 0.9 and 1.5‰ (Vance et al. 2008). δ^{65}Cu values of the Northeastern Pacific seawater increases gradually from 0.9‰ at the ocean surface to a maximum of approximately 1.3‰ at 100 m and then gradually decreases to approximately 0.8‰ at a depth of 400 m (Bermin et al. 2006). δ^{65}Cu values in deep seawater of the South Indian and North Pacific seawater are heavier than those in surface seawater and become heavier with the age of deep seawater because of preferential scavenging of the lighter isotope to Fe–Mn oxides (Takano et al. 2014).

Cu isotopes could provide insight into the mechanisms of metal cycling and oceanic mass balance, marine Fe–Mn nodules and crusts represent a major output of Cu from seawater to sediments, hence, the record of Cu isotopes in Fe–Mn deposits has caught much attention (Maréchal et al. 2000; Little et al. 2014a, b). Cu isotope compositions from 31 surface scrapings of global oceanic Fe–Mn nodules do not demonstrate significant differences (Fig. 3), and Cu isotopes do not display distinct geographical distributions, δ^{65}Cu changes between 0.05 and 0.6‰ and averages 0.31‰ ± 0.23‰ (Maréchal et al. 2000). Cu isotope analyses on the Fe–Mn crust D11-1 from the central Pacific, crust Alvin 539 from the North Atlantic, and crust 109D-C from the Indian Ocean show that δ^{65}Cu changes between −0.16‰ and +1.19‰. δ^{65}Cu in crust D11-1 has not changed since 17 Ma, which averages 0.54‰ ± 0.07‰. δ^{65}Cu in crust Alv539, with a mean of 0.33‰ ± 0.15‰, has changed slightly since 15 Ma. δ^{65}Cu in the crust 109D-C,

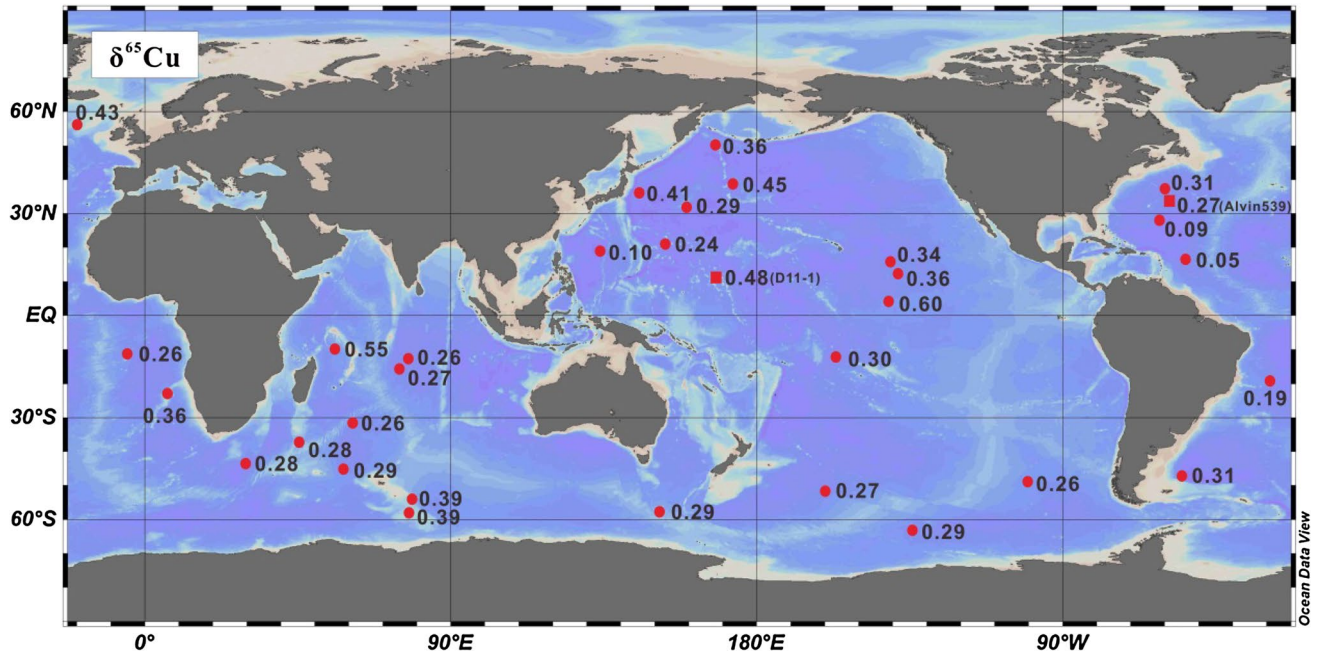

Fig. 3 Map of marine Fe–Mn nodules and crusts locations and δ^{65}Cu values of surface scrapings from each sample. Data from Maréchal et al. (2000), Little et al. (2014a)

decreased from +0.3 to +0.15‰ between 11 and 6 Ma. It is evident that Cu isotopes demonstrate differences among oceans but do not change significantly with time (Little et al. 2014a). Apparent isotope fractionation exists between Fe–Mn nodules/crusts and seawater in that Fe–Mn nodules/crusts contain lighter Cu isotopes (Maréchal et al. 2000; Little et al. 2014a). Little et al. (2014b) studied the fractionation mechanisms of Cu isotopes between Fe–Mn crusts and seawater using extended X-ray absorption fine structure (EXAFS). They believed that dissolved Cu in seawater mainly exists as hydrate $Cu(H_2O)_5^{2+}$ and tends to combine with strong organic ligands, which are more favourable of the heavy isotope ^{65}Cu. Consequently, the manganese oxides in the Fe–Mn nodules and crusts are more favourable of lighter Cu isotopes.

3.3 Zinc (Zn) isotopes

Zinc usually exists in the form of +2 valence in the lithosphere, hydrosphere, biosphere, and atmosphere. It widely participates in a variety of geochemical processes and life activities (Albarède 2004). Zinc is the second most abundant transition metal in the ocean, exhibiting a nutrient depth profile similar to those of biologically active major elements like nitrogen and phosphorus (Bruland 1989; Sinoir et al. 2012). Zn has five naturally occurring stable isotopes (Table 1): ^{64}Zn (48.63%), ^{66}Zn (27.90%), ^{67}Zn (4.10%), ^{68}Zn (18.75%), and ^{70}Zn (0.62%). Natural mass-dependent Zn-isotope variations span a range of ~ 1‰ amu^{-1}, usually expressed as δ^{66}Zn relative to the standard. There is no unified international standard for Zn isotopes, JMC 3-0749 and JMC-Lyon are widely used currently.

In global seawater, Zn concentrations range between 0.1 and 10 nM (Bermin et al. 2006), whereas 95% of Zn forms stable compounds with organic matter, and 5% exists in the form of free ions (Bruland 1989). The residence time of Zn in ocean is 11 kyr (Little et al. 2014a). Sources for oceanic Zn include river runoff, hydrothermal inputs, and atmospheric depositions, and the main sinks for Zn are Fe–Mn oxides, carbonate depositions and continental margin sediments (Little et al. 2014a, 2016). δ^{66}Zn values of the GA03 seawater vertical profile in the North Atlantic range from −1.10 to +0.90‰ (relative to JMC-Lyon standard). The top 100 m has the largest differences, with δ^{66}Zn ranging from −1.10 to +0.90‰, from 100 to 1000 m, it increases from −0.6‰ to +0.6‰, and below 1000 m, it is stable and averages +0.45‰ ± 0.24‰ (Conway and John 2014). On the seawater vertical profile from the SAFe station in the Pacific, the Zn concentration at 25 m is 0.7 nmol/kg, and δ^{66}Zn is −0.15‰ ± 0.06‰ (relative to JMC-Lyon standard). At 100 m, δ^{66}Zn is −0.05‰ ± 0.09‰. From 100 to 500 m, δ^{66}Zn increases with depth. Below 500 m, Zn concentrations reach 9 nmol/kg, and Zn isotope composition is stable between +0.45 and +0.56‰ (Conway and John 2015). The Zn isotope distribution in the North Pacific seawater depth profile is consistent with that of the SAFe station (Bermin et al. 2006). In the Southern Ocean, Zn concentrations increase with depth. δ^{66}Zn values change significantly in

the surface seawater over a range of 0.07–0.80‰ (relative to JMC 3-0749 L standard). Below 1000 m, similar to the North Atlantic and the North Pacific, δ^{66}Zn is stable and relatively uniform and averages 0.53‰ ± 0.14‰ (Zhao et al. 2014), which is also consistent with the fact that Zn has a very long residence time in the ocean. However, at the surface and the intermediate water, heavy Zn isotopes remain in seawater due to strong biological absorption, whereas light Zn isotopes are enriched within organisms (Conway and John 2014; Zhao et al. 2014).

It seems likely that the Zn isotopes could be useful in understanding the processes controlling water-column Zn distributions, and constraints on its global oceanic mass balance, and biogeochemical cycling of the metal in the modern ocean (Albarède 2004; Conway and John 2014; Zhao et al. 2014). Marine Fe–Mn sediments represent one of the largest sinks from global seawater for Zn (Maréchal et al. 2000; Juillot et al. 2008; Little et al. 2014a, b; Bryan et al. 2015). Zn isotopes were analysed systematically from 40 surface scrapings of Fe–Mn nodules from global oceans and Fe–Mn crust profiles from three oceans (Fig. 4). Zn isotope compositions on the global Fe–Mn nodules surface demonstrate a large range of variations of 0.53–1.16‰ for δ^{66}Zn and an average of 0.90‰ ± 0.28‰ (relative to JMC 3-0749 L standard). Variations of Zn isotopes in Fe–Mn nodules highly depend on latitude, Zn isotopes in the tropical oceans are relatively lighter, whereas those in the polar oceans are relatively heavier (Maréchal et al. 2000). Zn isotope analyses on the Fe–Mn crust D11-1 from the Central Pacific, crust Alvin539 from the North Atlantic, and crust 109D-C from the Indian Ocean show that δ^{66}Zn changes between 0.6 and 1.13‰ and averages 1.04‰ ± 0.21‰ (relative to JMC-Lyon standard). δ^{66}Zn in crust D11-1, which averages 1.12‰ ± 0.12‰, has slight variations since 17 Ma; δ^{66}Zn in crust Alv539 has a small change since 15 Ma and its average of 0.96‰ ± 0.17‰; δ^{66}Zn from crust 109D-C, which averages 0.97‰, is similar to that from the other two crusts and has not changed much (Little et al. 2014a). Apparently, these studies have observed that Zn isotopes in Fe–Mn nodules and crusts are consistent and demonstrate significant isotopic fractionation with seawater, and a significant enrichment of heavy Zn isotopes in Fe–Mn deposits, moreover, the adsorption reactions at mineral/water interfaces are thought to result in mass-dependent fractionation of Zn isotopes throughout the water column. Some experimental studies explained the mechanism responsible for preferential enrichment of heavy isotopes of Zn in Fe–Mn nodules and crusts. Juillot et al. (2008) revealed an equilibrium fractionation mechanism with an enrichment of heavy Zn isotopes during adsorption onto 2-Line ferrihydrite and goethite. Two minerals perform differently vis-à-vis the absorption and fractionation of Zn isotopes. These different magnitudes of Zn fractionation are related to structural differences between Zn complexes existing on the surface of goethite (octahedrally coordination) and ferrihydrite (tetrahedrally coordination) (Schauble 2004; Ponthieu et al. 2006). Utilizing EXAFS analysis, Little et al. (2014b) believed that the combination of Zn with birnessite in Fe–Mn crusts is

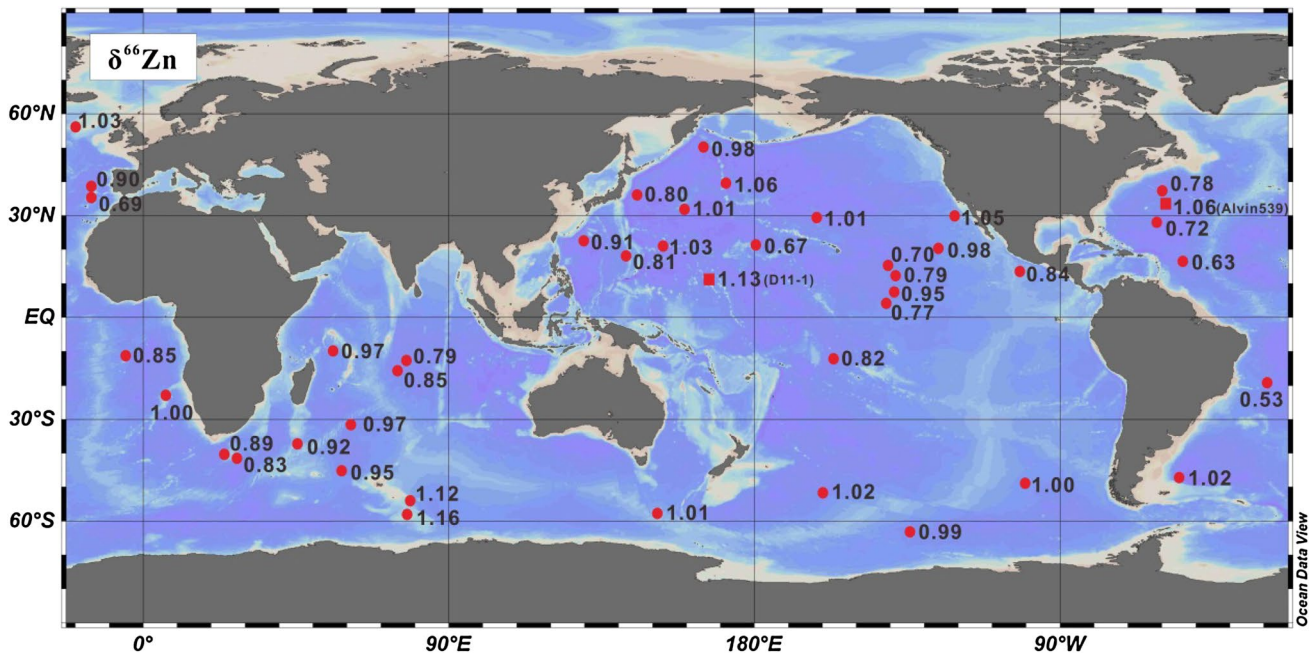

Fig. 4 Map of marine Fe–Mn nodules and crusts locations and δ^{66}Zn values of surface scrapings from each sample. Data from Maréchal et al. (2000), Little et al. (2014a)

through the tetrahedral coordination, whereas Zn in seawater usually combines in the form of $Zn(H_2O)_6^{2+}$ through octahedral coordination. Therefore, different from the Cu isotopes, Zn isotopic fractionation between Fe–Mn deposits and seawater is inorganic fractionation during the absorption of Zn by manganese oxide minerals. Bryan et al. (2015) conducted experiments at different ionic strength and different surface loading, they found that Zn was adsorbed to birnessite firstly as tetrahedral complexes at low surface loading, with preferential incorporation of heavier isotopes relative to the octahedral Zn species predominating in solution at a high ionic strength. As surface loading increases, so does the percentage of Zn adsorbing as octahedral complexes, thus diminishing the magnitude of fractionation between the dissolved and adsorbed pools of Zn.

3.4 Molybdenum (Mo) isotopes

Molybdenum, which has unique chemical behaviour, is a typical redox-sensitive element. The Mo element and its isotopes have played a key role in constraining the chemical environments of ancient oceans. Mo has seven naturally occurring stable isotopes (Table 1): ^{92}Mo (14.84%), ^{94}Mo (9.25%), ^{95}Mo (15.92%), ^{96}Mo (16.68%), ^{97}Mo (9.55%), ^{98}Mo (24.13%), and ^{100}Mo (9.63%) (Anbar 2004). Natural mass-dependent Mo isotope variations span a range of ~ 1‰ amu^{-1} mass difference. Early reports on Mo isotopes mostly expressed as $\delta^{97/95}$Mo, whereas $\delta^{98/95}$Mo is now widely taken due to the double isotope dilution method. There is presently no international Mo reference standard, data are typically reported relative to in-house laboratory standards include NIST SRM 3134, JMC Mo, MOMO and Alfa Aesar Mo, which produce consistent Mo isotope composition results with tolerable errors for comparisons.

In modern oxic seawater, Mo is dissolved as molybdate (MoO_4^{2-}) species with concentrations reaching 10.3 ± 0.48 µg/L (or 107 nM) (Collier 1985). The high concentration of Mo in the modern oceans is largely dictated by the high solubility of Mo phases and slow removal rate of MoO_4^{2-} in the presence of dissolved O_2. Mo has a long residence time in the ocean, probably 400 kyr (Miller et al. 2011) but possibly as long as 800 kyr (Firdaus et al. 2008), with several orders of magnitude greater than ocean mixing times. In the oceans, the source for Mo is the riverine inputs and low-temperature hydrothermal inputs, quantitatively, the latter of which is approximately 10% of the former inputs (Miller et al. 2011). The sinks of oceanic Mo are mainly authigenic Fe–Mn oxides and anoxic sediments, and depend on the redox degree of the seawater. In oxygenated settings, removal of Mo from the water column leads to strong Mo enrichments in Fe–Mn crusts and nodules, such enrichment most likely reflects authigenic accumulation of Mo by adsorption to and/or co-precipitation with Mn oxides (Barling and Anbar 2004). In euxinic settings, molybdate (MoO_4^{2-}) is converted to sulfur-containing Mo complexes (e.g., thiomolybdate or Mo polysulfide) in H_2S-bearing systems (Erickson and Helz 2000; Dahl et al. 2013). Regarding the Mo isotope composition of seawater, Barling et al. (2001) reported Pacific seawater $\delta^{97/95}$Mo as 1.48‰ ($\delta^{98/95}$Mo = 2.22‰). Siebert et al. (2003) tested seawater samples obtained from the Atlantic, the Pacific, the Indian oceans and the Labrador Sea and showed that their $\delta^{98/95}$Mo ranged from 2.3 to 2.5‰ and a mean of 2.3‰ ± 0.1‰ (relative to JMC standard). These studies illustrate that seawater from different oceans over the globe has the same Mo concentration (0.011 ppm) and uniform Mo isotope composition.

According to its redox-sensitive character, the abundance and isotope composition of Mo recorded in sediments are frequently used as proxies to reconstruct the redox evolution of the oceans and atmosphere (Barling et al. 2001; Siebert et al. 2003; Barling and Anbar 2004; Kurzweil et al. 2015). Scholars investigated different types of marine Fe–Mn oxides from different oceans and explored the possibility of Mo stable isotope geochemistry in paleoredox applications (Barling et al. 2001; Siebert et al. 2003; Goto et al. 2015). Barling et al. (2001) performed Mo isotope analysis on Fe–Mn nodule standard materials NOD-P-1 and NOD-A-1 obtained from the Pacific and Atlantic, and the results show that $\delta^{98/95}$Mo values (relative to JMC standard) are −0.63‰ ± 0.1‰ and −0.95‰ ± 0.1‰, respectively, which demonstrate the characteristics of enriched light Mo isotopes and significant isotopic fractionation from seawater (2.3‰). This phenomenon may be attributed to the oxidized environment, in which the absorption of Mo onto ferromanganese oxides and hydroxides tends to enrich lighter Mo isotopes, which leads to heavy Mo isotopes in seawater and an isotopic fractionation of 2‰ between seawater and ferromanganese oxides/hydroxides. Siebert et al. (2003) performed Mo isotope analysis on two profiles of Fe–Mn crusts (BM1969.05 and 237KD) and six Fe–Mn crust surface scrapings from three oceans. $\delta^{98/95}$Mo values (relative to JMC standard) of the two profiles range from −0.5 to −1.0‰ and from −0.6 to −0.7‰, respectively. $\delta^{98/95}$Mo data from 6 surface samples are also very stable between −0.5 and −0.8‰. These Mo isotope ranges are consistent with the results from Barling et al. (2001). Therefore, Mo isotope compositions of the seawater from various ocean basins and depths are homogeneous, whereas Mo isotope compositions in Fe–Mn crust have not changed significantly since 60 Ma. In addition, Goto et al. (2015) analysed the Mo isotope in the modern marine hydrothermal manganese crusts collected from the Ryukyu arc system. Their results show that the hydrothermal manganese crusts have high concentrations of Mo. The $\delta^{98/95}$Mo range is −0.56 to −0.66‰ (relative to NIST SRM 3134 standard), which is

lighter than the Mo isotope of hydrothermal fluids (~0.5‰; McManus et al. 2002) and modern seawater, and similar to that of hydrogenetic Fe–Mn nodules and crusts. Although the possible contribution of hydrothermally derived Mo cannot be excluded, such light Mo isotopes may mainly come from the isotopic fractionation induced by the changes in coordination number during the adsorption of Mo from seawater onto Mn oxides. The Mo isotopic fractionation caused by the absorption onto ferromanganese oxides/hydroxides has been verified by subsequent absorption experiments. Laboratory studies have shown that the lighter ^{95}Mo isotope is preferentially adsorbed by minerals compared to ^{97}Mo, with a fractionation of about 2‰ (Barling and Anbar 2004; Goldberg et al. 2009), and the fractionation is greatest when there is a large change in the structure of the sorbed ion, e.g. a change from tetrahedral to octahedral coordination such as occurs when MoO_4^{2-} is adsorbed to MnO_2 (Wasylenki et al. 2011; Kashiwabara et al. 2011). Much smaller isotopic fractionations have been observed when there is no change in coordination, as with ferrihydrite (Goldberg et al. 2009; Kashiwabara et al. 2011).

3.5 Thallium (Tl) isotopes

Thallium has both lithophile affinity and sulphophile affinity and is therefore highly decentralized in the crust, with an average abundance of only 0.75×10^{-6} (Taylor and McLennan 1985). Tl has two naturally occurring isotopes (Table 1): ^{203}Tl (29.5%) and ^{205}Tl (70.5%). This equates to a relative mass difference of < 1%. Tl isotope is usually expressed as ε^{205}Tl ($\varepsilon^{205/203}$Tl) relative to the international standard NIST SRM 997.

In the ocean, Tl has a residence time of 18.5 kyr, which is larger than the ocean mixing time and a conservative distribution (Flegal and Patterson 1985; Rehkämper and Nielsen 2004). Flegal and Patterson (1985) performed accurate comparisons of seawater Tl concentrations from different locations of the oceans (the North and South Pacific and the deep water and surface water of the Pacific and Atlantic). Their results show that seawater Tl concentration is distributed quite uniformly between 12 and 16 pg/g and averages 13.3 pg/g. Previous scholars have various understandings of the dissolved form of Tl in seawater. Batley and Florence (1975) found that in the Pacific Tl mainly exists as Tl^{3+}, which accounts for 80% of total Tl, whereas Tl^{+} only accounts for 20%. This may be due to the variety of complex ligands and colloidal substances in seawater. Nielsen et al. (2009) believed that Tl in seawater mainly exists in the forms of Tl^{+} and TlCl. Oceanic Tl has 5 input fluxes, which are rivers (1.3 Mmol/year), hydrothermal fluids (1.2 Mmol/year), subaerial volcanism (1.6 Mmol/year), mineral aerosols (0.4 Mmol/year), and benthic fluxes from continental margins (0.7 Mmol/year). The output fluxes of Tl include pelagic clays (1.3 Mmol/year) and altered oceanic crust (2.9 Mmol/year) (Rehkämper and Nielsen 2004; Nielsen et al. 2006). Previous studies have performed Tl isotope tests on seawater from various oceanic locations. Samples from Tenerife Island in the North Atlantic have light ε^{205}Tl of approximately −8.1. Seawater at different depths in the Arctic Ocean has consistent Tl isotope composition with ε^{205}Tl approximately −5.5. Tl isotopes from the Atlantic and Arctic Oceans have some minor differences, which may be attributed to the different regional continental inputs (Rehkämper et al. 2002). The ε^{205}Tl range for the South Atlantic is −5.8 to −6.3, with a relatively consistent Tl isotope composition that averages -6.0 ± 0.3 (Owens et al. 2017). In general, global seawater has relatively light and uniform Tl isotope compositions that average -5.8 ± 0.6 (Rehkämper et al. 2002; Owens et al. 2017).

The marine Tl isotope geochemistry is of interest because it could respond to important changes in ocean chemistry such as cycling of Fe and Mn, bottom water oxygen conditions as well as marine organic carbon burial (Baker et al. 2009; Nielsen et al. 2009). Tl isotopes recorded in marine Fe–Mn crusts show great promise as a tracer of past changes in Earth's marine and climatic conditions (Rehkämper et al. 2004; Baker et al. 2009; Nielsen et al. 2009). Up to the present, Tl isotopes of Fe–Mn nodules and crusts have been extensively studied mainly by the research group of Rehkämper and Nielsen. Tl isotope compositions of hydrogenetic Fe–Mn crusts, diagenetic Fe–Mn nodules and hydrothermal manganese sediments demonstrate significant differences and systematic variations (Fig. 5) (Rehkämper et al. 2002, 2004; Nielsen et al. 2009, 2011, 2013). The surface scrapings of globally hydrogenetic Fe–Mn crusts have uniform Tl isotope compositions, and are enriched in heavy Tl isotopes, with ε^{205}Tl between +10 and +14.5, implying a constant equilibrium isotope fractionation between seawater and Tl incorporated into the Fe–Mn crusts (Rehkämper et al. 2002; Nielsen et al. 2013). Peacock and Moon (2012) confirmed this conclusion with absorption experiments and high accuracy measurements of X-ray absorption spectroscopy (XAS). The results show that Tl(I) is oxidized into Tl(III) when absorbed into the hexagonal birnessite. Tl(III) forms an inner-sphere complex at the hexagonal birnessite surface, located at vacant octahedral sites in the phyllomanganate sheets. It is noteworthy that Tl(I) only forms surface complex but is not oxidized when absorbed on todorokite, triclinic birnessite, and ferrihydrite. The diagenetic-hydrogenetic deep-water Fe–Mn nodules and crusts exhibit a much large ranges of variation in ε^{205}Tl (0 to +9), whereas the shallow-water diagenetic deposits from the Baltic Sea demonstrate variations ranging over −5 to 0, indicating that Tl absorption may occur in a closed-system reservoir of limited size in which pore fluids stagnate and absorption is fast. Hydrothermal manganese sediments are similar to

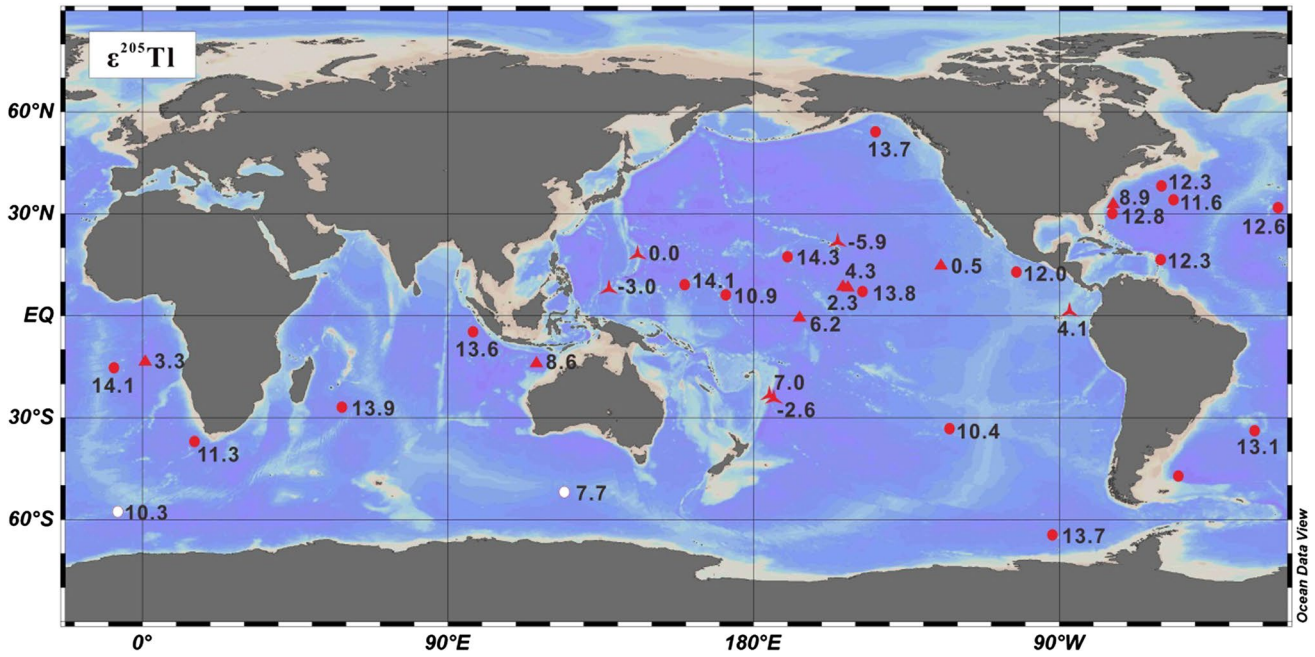

Fig. 5 Map of marine Fe–Mn nodules and crusts locations and ε^{205}Tl values of surface scrapings from each sample. Data from Rehkämper et al. (2002). The solid red circles represent hydrogenetic deposits, the red triangles represent the deep-water diagenetic deposits, the triangle stars represent hydrothermal manganese deposits, and the empty circles represent mixed hydrothermal–hydrogenetic deposits

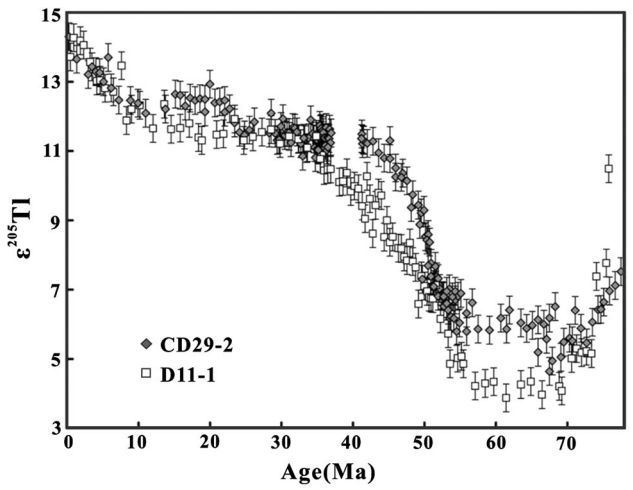

Fig. 6 Time-series of the Tl isotope composition of Pacific Fe–Mn crusts D11-1 and CD29-2. Data and figure are from Nielsen et al. (2009)

diagenetic manganese sediments, ε^{205}Tl ranges of which are between those of seawater and hydrogenetic Fe–Mn deposits (Rehkämper et al. 2002).

Some studies have established Tl isotope depth profiles for several marine Fe–Mn crusts, and identified large systematic variations in Tl isotope compositions (Fig. 6) (Rehkämper et al. 2004; Nielsen et al. 2009, 2013). Rehkämper et al. (2004) determined the first depth profiles of Tl isotopes in Fe–Mn crusts from the Atlantic, Pacific, and Indian Oceans. In three crusts older than 25 Ma, from 60 to 25 Ma, ε^{205}Tl increases with the crust ages decreases. Especially over 55 ~ 40 Ma, ε^{205}Tl increases dramatically from + 6 to + 12, which may be due to the changes in the Tl isotope composition of seawater that were caused by changes in the marine input and/or output fluxes of Tl element during the Early Cenozoic. Nielsen et al. (2009) presented high resolution Tl isotope records in two Fe–Mn crusts, CD29-2 and D11-1 from the Pacific Ocean (Fig. 6). The result shows that Tl isotope curve of Cenozoic seawater has a significant ε^{205}Tl changes and there is a large shift in the ε^{205}Tl value between 55 and 45 Ma, it reflects an increase in organic carbon export in the oceans, which led to a decrease in the amount of authigenic Fe–Mn oxides that were deposited with pelagic sediments in the early Eocene. Time-dependent variations of Tl isotope compositions in Fe–Mn crusts can be interpreted to reflect either changes in the isotope fractionation factor between seawater and Fe–Mn crusts or the Tl isotope composition of seawater (Rehkämper et al. 2004; Nielsen et al. 2009). Factors that potentially influence the fractionation factor need to be further explored and the Tl isotope compositions of the main sources and sinks of dissolved oceanic Tl need to be further investigated.

3.6 Cadmium (Cd) isotopes

Cadmium is a highly volatile, chalcophile, moderately incompatible and biologically active trace element with a single oxidation state (Cd^{2+}) in the Earth (McDonough and Sun 1995). Cd concentrations in Fe–Mn nodules and crusts range between 2 and 20 ppm, which are significantly higher than its abundance in the crust (0.2×10^{-6}) (Hein 2004; Hein and Koschinsky 2014). Cd has eight naturally occurring stable isotopes (Table 1): ^{106}Cd (1.25%), ^{108}Cd (0.89%), ^{110}Cd (12.49%), ^{111}Cd (12.80%), ^{112}Cd (24.13%), ^{113}Cd (12.22%), ^{114}Cd (28.73%) and ^{116}Cd (7.49%), with a large (> 9%) relative mass difference, which could lead to large mass-dependent isotope fractionation. According to the abundance of Cd isotopes and its interferences with isotopes of other elements, $\varepsilon^{114/110}$Cd is widely used internationally to characterize Cd isotopes. To date, there is no unified international standard for Cd isotope analysis. Alfa Cd Zürich, NIST SRM 3108, JMC Cd Mainz and JMC Cd Münster are widely used for research.

The major natural sources of Cd are injected into the ocean by atmospheric deposition, rivers and hydrothermal activity, whereas the sinks are absorption by organisms, sediments, and Fe–Mn oxides (Simpson 1978; Collier and Edmond 1984; Rosenthal et al. 1995). Previous study has shown that although the residence time of Cd in seawater (50 kyr) is larger than the mixing time of seawater, Cd is not homogenous in the oceans (Bewers and Yeats 1977). Previous Cd isotope analyses on seawater depth profile samples from various locations in the Pacific, Atlantic, Arctic, and the Southern Ocean show that Cd concentrations and isotope compositions differ significantly at different depths or different locations. The fractionation has the tendency of variation with water depth and latitude (Lacan et al. 2006; Ripperger et al. 2007; Xue et al. 2013; Conway and John 2015). Ripperger et al. (2007) showed that seawater samples from above 150 m in each ocean display large ranges of Cd isotope compositions, the $\varepsilon^{114/110}$Cd (relative to NIST SRM 3108 standard) of which are between − 6.8 and + 37. Most samples have low concentrations of Cd (< 0.03 nmol/kg). Samples below 900 m have more enriched Cd (0.3–0.9 nmol/kg) and relatively consistent Cd isotope compositions ($\varepsilon^{114/110}\text{Cd} \approx +2.5$, relative to NIST SRM 3108 standard) (Ripperger et al. 2007). Conway and John (2015) found similar characteristics in the seawater from the SAFe station in the Pacific Ocean. Below 500 m, $\varepsilon^{114/110}$Cd is approximately + 3 (relative to NIST SRM 3108 standard). Approaching the surface, Cd isotopes become increasingly heavier. At 35 m, $\varepsilon^{114/110}$Cd is approximately + 8.5, indicating that Cd isotopes in shallow water are mainly influenced by biological absorption. The oceanic Cd concentrations and isotopes demonstrate correlations below certain depths. Most seawater samples have negative correlations between Cd isotope ratio and dissolved Cd concentration, which reflects the dynamical isotopic effects of Cd absorption by phytoplankton in a closed system. Oceanic Cd isotopes are mainly controlled by water body mixing, phytoplankton absorption, and anthropogenic inputs (Lacan et al. 2006; Ripperger et al. 2007; Ripperger and Rehkämper 2007; Xue et al. 2013).

From the above, it is likely that Cd isotope data for seawater can provide insights into the cycling of this element in the marine environment. As a valuable paleoceanographic document, there is important significance to test the potential of Fe–Mn crusts to monitor seawater Cd isotope variations. Such an archive will be useful to further investigate the marine biogeochemical cycling of Cd and the application of Cd isotopes as a proxy for nutrient utilization. Schmitt et al. (2009) performed a Cd isotopic analysis on 31 hydrogenetic Fe–Mn nodule surface scrapings worldwide and a hydrogenetic Fe–Mn crust (121DK) depth profile from the Northeastern Atlantic. Their analysis showed that $\varepsilon^{112/110}$Cd (relative to JMC Cd Mainz standard) in the hydrogenetic Fe–Mn sediments ranges between − 0.54 and + 2.0 (converted into the $\varepsilon^{114/110}$Cd relative to NIST SRM 3108 is between 0.39 and 5.43). Samples from above 2000 m had heavier Cd isotopes compared to samples from deep waters, which reflects shallow inorganic scavenging of Cd by Fe–Mn oxides and its remineralization at depth. Cd isotope composition in the shallow water Fe–Mn nodules is consistent with the seawater Cd isotope compositions measured by Ripperger et al. (2007), which indicate that precipitation of Fe–Mn oxides from seawater only produces very limited Cd isotope fractionation. Relatively heavy Cd isotopes in shallow water samples are due to Cd absorption by phytoplankton. Cd isotope changes recorded in Fe–Mn crust 121DK from the Northeastern Pacific reveal that the oceanic Cd circulation has not experienced significant long-term changes since 8 Ma, and thus $\varepsilon^{112/110}$Cd can be used as a proxy of paleo-productivity for a specific depth in the oceans (Schmitt et al. 2009). Horner et al. (2010) analysed the Cd isotopes of 15 Fe–Mn crust surface scrapings from the Atlantic, Pacific, Indian, and the Southern Ocean (14 samples from below 900 m). With the exception of one sample (DR 153), all samples display a narrow range of Cd isotope compositions between $\varepsilon^{114/110}$Cd (relative to Alfa Cd Zürich) values of 1.8–4.6 (converted to NIST SRM 3108 is between 0.67 and 3.46), which is consistent with Cd isotope compositions in seawater below 900 m (Ripperger et al. 2007). Therefore, deep water Fe–Mn crusts and seawater do not demonstrate significant isotopic fractionation and thus can be used to record the Cd isotope composition of seawater.

3.7 Lithium (Li) isotopes

Lithium, the lightest of the alkali elements, exists mainly in the form of +1 valence and demonstrates high environmental activity. It has small abundance but is distributed widely on Earth. Li has two naturally occurring stable isotopes (Table 1): ^{6}Li (7.5%) and ^{7}Li (92.5%). They have a large mass difference (16.7%), resulting in a significant mass dependent fractionation. Consequently, the range in lithium isotope ratios observed in terrestrial samples is enormous, up to ± 100‰ (Tomascak 2004). This large fractionation provides enormous potential for application of lithium isotopes as a geochemical tracer. Similar to other non-traditional isotopes, Li isotopes commonly expressed as δ^{7}Li ($\delta^{7/6}$Li) relative to the international standard NIST L-SVEC (SRM 8545).

The high solubility of Li means that it is a conservative element in the oceans. It has a long residence time of approximately 1.2 Ma (Huh et al. 1998). The dominant sources of dissolved Li to seawater are rivers (10×10^{9} mol/year), hydrothermal inputs (13×10^{9} mol/year), and subduction reflux (6×10^{9} mol/year) (Huh et al. 1998). The removal of Li from seawater is entirely by incorporation into marine sediments and low-temperature altered oceanic crust (Misra and Froelich 2012). Li concentrations in seawater are quite homogeneous vertically and laterally at approximately 175 ppb. Li isotope compositions at different locations in the global ocean differ slightly, with δ^{7}Li ranging from 29.3 to 33.3‰. The average δ^{7}Li is 31.13‰ for the Pacific, 31.12‰ for the Mediterranean, 31.17‰ for the North Atlantic, and 30.75‰ for the Sargasso Sea (Chan and Edmond 1988; Tomascak 2004; Misra and Froelich 2009; Millot et al. 2004). Previous studies constructed Li isotope history of Cenozoic seawater by analysing planktonic foraminifera, the δ^{7}Li value of seawater rose by 9 per mil (‰) from the Paleocene to the present (Misra and Froelich 2012).

The lithium isotope of seawater incorporated into Fe–Mn crusts has the potential to record changes in seawater chemistry, help unravel the changing factors linked to continental weathering, hydrothermal circulation and alteration of oceanic crust (Tomascak 2004; Chan and Hein 2007; Misra and Froelich 2012). To establish the validity of Fe–Mn crusts as a recorder of seawater δ^{7}Li, Chan and Hein (2007) measured the Li contents and isotope compositions of 32 Fe–Mn crusts from a variety of tectonic environments in the global ocean. Their results showed that Li tends to exist in hydrothermal crusts rather than hydrogenetic crusts. Therefore, Li concentrations can be used to trace the sources of related deposits and can be used as a sensitive indicator of the history of local hydrothermal activity. Chan and Hein performed step leaching experiments on these various types of Fe–Mn deposits with HAc and HCl. They separated the loosely bound Li via HAc (HAc-Li) and the more tightly bound Li via HCl (HCl-Li). The results show that HAc-Li δ^{7}Li in hydrogenetic and hydrothermal crusts are similar to the Li isotope in modern seawater, whereas HCl-Li δ^{7}Li is relatively lighter, indicating that Li is incorporated in the crystal lattices of Mn–Fe oxides–oxyhydroxides by inner sphere complexation with preference for ^{6}Li. The research also found that due to the high mobility of Li, the initial characteristic of Li isotopes in Fe–Mn crusts changes after sedimentation and exchanges with seawater and thus cannot be used to record the long-term evolution of seawater Li isotopes.

3.8 Magnesium (Mg) isotopes

Magnesium is the 8th most abundant element in the continental crust and the 4th most abundant species in seawater (Taylor and McLennan 1985), and it is the second most abundant cation in the ocean (1276 ppm), following Na (Edmond et al. 1979). Mg participates in almost all geochemical processes on Earth. Mg has three naturally occurring stable isotopes (Table 1): ^{24}Mg (78.99%), ^{25}Mg (10.00%) and ^{26}Mg (11.01%). Mg isotopes commonly expressed as δ^{26}Mg relative to the international standard DSM-3. The standard SRM980 has been temporarily abandoned due to its nonuniformity (Galy et al. 2003).

In the oceans, Mg primarily exists in the form of Mg^{2+} ions (or the hydrate $Mg(H_2O)_6^{2+}$). The input fluxes of oceanic Mg are rivers and groundwater (5.2×10^{12} mol/year), for which rivers account for a large portion, whereas groundwater may only account for approximately 10% of the continental total inputs (Wilkinson and Algeo 1989; Berner 2004). The output fluxes of Mg are exchange with the oceanic crust during hydrothermal circulation at mid-ocean ridges (0.5×10^{12}–2×10^{12} mol/year), the precipitation of dolomite (0.1×10^{12}–0.8×10^{12} mol/year), and ion-exchange reactions with clays (Elderfield and Schultz 1996; Tipper et al. 2006). Previous studies have measured Mg concentrations and isotope compositions of seawater at various locations. Their results illustrate a relatively uniformed Mg concentration (53 mmol/L) and isotope composition ($\delta^{26}Mg = -0.82$‰) in modern oceans (Young and Galy 2004; de Villiers et al. 2005; Tipper et al. 2006), which is consistent with the long residence time of Mg in the ocean (~ 13 Ma; Berner and Berner 1987) and indicates that Mg has fully mixed in the oceans so that its isotopes are evenly distributed.

Mg isotope records can be used to quantify the relative contributions of changes in silicate or carbonate fluxes to the global Mg budget (Young and Galy 2004; Tipper et al. 2006). Although marine Fe–Mn nodules and crusts are not allimportant Mg sinks in seawater, Mg isotopes in Fe–Mn deposits may be likely to provide important paleoceanographic information, such as seawater Mg isotope record and seawater Mg budget. Until now, very few research efforts

have been achieved in Mg isotope studies of Fe–Mn nodules and crusts. Rose-Koga and Albarede (2010) tested the Mg isotopes from 26 Fe–Mn nodules surface scrapings from the global oceans. Their results showed that Mg isotopes of Fe–Mn nodules from different oceans have significant differences. δ^{26}Mg in the Pacific and Atlantic Fe–Mn nodules display a small range of −1.89 to −0.54‰, whereas those from the Indian Ocean display a large range of −2.94 to +0.69‰. Mg isotope compositions in Fe–Mn nodules and seawater are also different. Rose-Koga et al. explained that Mg isotopic fractionation is produced by the difference of early oxic diagenesis. Since Mg is an important petrogenic element, and its abundance in ocean ranks 2nd after Na, the occurrence state of Mg in Fe–Mn nodules and crusts is different from that of Mo, Cu, and Zn. Due to the various occurrence states of Mg in Fe–Mn crusts, Fu and Wang (2012) performed sequential step-leaching experiments and showed that the main occurrence states of Mg in Fe–Mn crusts are exchangeable Mg, Mg bound to carbonates, Mg bound to Fe–Mn oxides. The remaining states account for less. Fu et al. (unpublished data) found that the surface of Fe–Mn crust MP2D06 from Central Pacific has a δ^{26}Mg of −1.55‰ in exchangeable Mg, −1.12‰ in Mg bound to carbonates, +1.01‰ in the Fe–Mn oxides. δ^{26}Mg value in Fe–Mn oxides is relatively heavy and has a significant fractionation with modern seawater (−0.82‰) (Young and Galy 2004; Tipper et al. 2006). Mg isotope compositions in various occurrence states in Fe–Mn crusts demonstrate isotope fractionation controlled by minerals. δ^{26}Mg in the Fe–Mn oxides at depth profile of Fe–Mn crust MP2D06 display a large variations, which may be the result of changes in the Mg isotope composition of seawater and/or the changes in fractionation coefficient between Fe–Mn crusts and seawater. So far, the use of Mg isotopes in Fe–Mn deposits as a tool in research of seawater Mg isotope record and seawater Mg budget is currently limited by scant data. Therefore, measurements of the Mg isotopic composition of Fe–Mn nodules and crusts should be further explored in future studies.

3.9 Nickle (Ni) isotopes

Nickle is a nutrient element in the oceans. Its circulation is related to biogeochemical processes (Cameron et al. 2009). Ni has five naturally occurring stable isotopes (Table 1): ^{58}Ni (68.08%), ^{60}Ni (26.22%), ^{61}Ni (1.14%), ^{62}Ni (3.63%) and ^{64}Ni (0.93%) (Gramlish et al. 1989). Ni isotopes are usually expressed as δ^{60}Ni ($\delta^{60/58}$Ni) relative to the SRM 986 international standard.

Worldwide, the concentration of Ni in seawater varies between approximately 2 and 12 nmol/kg, with a global average of 8.2 nmol/kg (Saager et al. 1992, 1997; Frew et al. 2001; Mackey et al. 2002; MBARI 2012; Cameron and Vance 2014). Dissolved Ni in seawater has three main sources: 40% from continental weathering products inputs via river and groundwater, 40% from the mineral dust and volcanic ash via the atmosphere, and 20% from hydrothermal vent fluids. The sinks for oceanic Ni are pelagic sediments and Fe–Mn deposits (Gaillardet et al. 2003; Li and Schoonmaker 2003; Gall et al. 2013). The residence time for oceanic Ni is controversial. Some scholars estimated it as 10 kyr (Sclater et al. 1976) while others estimated it as approximately 30 kyr (Cameron and Vance 2014) or 4 kyr (Li and Schoonmaker 2003; Rehkämper and Nielsen 2004). Previous studies have investigated the Ni isotope compositions in the North Atlantic, NE Pacific and the Southern Ocean. Their results showed that seawater has consistent Ni isotope composition, with δ^{60}Ni of 1.44‰ ± 0.15‰ (Gall et al. 2013; Cameron and Vance 2014).

The isotope composition of Ni in marine systems has recently attracted significant attention owing to its nutrient-type behavior and multiple sources in seawater (Gall et al. 2013; Cameron and Vance 2014; Little et al. 2015). Due to Fe–Mn deposits is a major sink of Ni in the oceans, scholars have attempted to establish Ni isotopic variability in Fe–Mn crusts and determine whether the crusts can be used as archives for deep water Ni isotope compositions (Gall et al. 2013; Gueguen et al. 2016). δ^{60}Ni in the Fe–Mn crust surface scrapings ranges from 0.9 to 2.5‰ and averages 1.6‰ ± 0.8‰, there was a consistent Ni isotope composition in different ocean basins. Compared with seawater, Fe–Mn crusts have heavier Ni isotopes (Gall et al. 2013; Gueguen et al. 2016). The isotopic fractionation between Fe–Mn crusts and seawater may be related to changes in Ni inputs via continental weathering and hydrothermal fluids but not related to the Ni adsorption and incorporation into Fe–Mn crusts (Gall et al. 2013). In addition, the North and South Pacific crusts have had very consistent Ni isotope compositions since 17 Ma despite different growth rates, textures and geochemical patterns (Fig. 7). δ^{60}Ni values on the 76 Ma crust CD29-2 depth profile from the Central Pacific display a large variation range of 1.6–2.3‰ (Fig. 7). Although the redistribution of Ni associated with phosphatisation may exist in older parts of the crust, there is no systematic difference in Ni isotopic composition between older parts and younger parts of the crust, which suggests a steady state of the oceanic Ni fluxes over the Cenozoic. Besides, changes in Ni isotopes in the crust profile are consistent with changes in Mn concentrations, implies that Ni isotopes in Fe–Mn crusts are related to Ni release via hydrothermal activity. Therefore, Ni isotope variations in Fe–Mn crusts may not only record the changes in oceanic Ni sources, but also post-depositional processes.

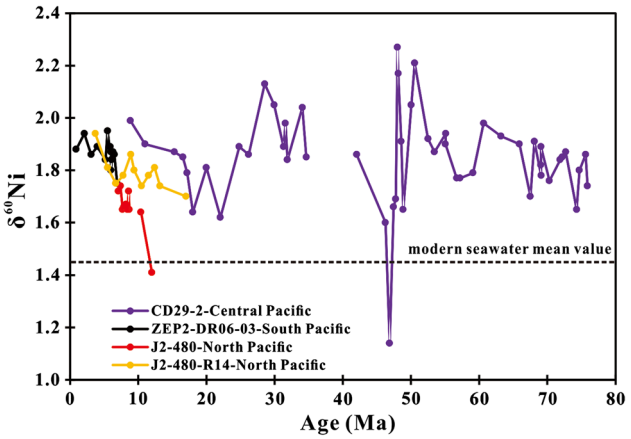

Fig. 7 Temporal δ^{60}Ni record from selected marine Fe–Mn crusts. The South Pacific Fe–Mn crust ZEP2-DR06-03 and North Pacific Fe–Mn crusts J2-480 and J2-480-R14 profiles are from Gueguen et al. (2016), the Central Pacific Fe–Mn crust CD29-2 profile is from Gall et al. (2013). The model age of crust CD29-2 is from Nielsen et al. (2009)

4 Summary and outlook

Marine Fe–Mn crusts and nodules have long been characterized for their elevated concentrations of metals (e.g., Co, Ni, Cu and Zn). Due to the slow growth rates (1–10 mm/Myr), they are condensed stratigraphic sections and, depending on their thickness, up to 70 Ma of oceanic history may be recorded in their layers. With the development of analytical instruments and methods, non-traditional stable isotopic geochemistry (e.g., Fe, Cu, Zn, Mo, Cd, Tl, Li and Mg) has experienced dramatic advancements. The past decade has seen an explosion of interest in the use of non-traditional stable isotopes for investigating marine processes and element cycling. The isotopic compositions of these metals in marine Fe–Mn crusts and nodules could offer the way to understand their enrichment mechanisms and mechanisms that control changes in Fe–Mn crust and nodule compositions with location in the global ocean. Meanwhile, they could provide interesting proxies to unravel changes in the marine sources and biogeochemical cycles of some metals through time as well as past chemical and isotopic compositions of various elements dissolved in oceanic deep water.

For these purposes, both the global variations of isotope ratios in Fe–Mn crusts and nodules surface scrapings and detailed depth profiles through the crusts were systematically investigated. These studies established non-traditional isotopic variability present in Fe–Mn crusts and nodules, explored the isotopic fractionation mechanisms associated with the Fe–Mn deposits formation, and determined whether these Fe–Mn crusts can be used as archives for deep water isotope compositions and long-term seawater isotope record. More importantly, non-traditional isotope compositions of marine Fe–Mn deposits have been successfully applied to constrain the metal sources and metal geochemical cycles in the ocean, understand continental weathering and climate change, and reconstruct paleo-oceanic redox conditions and past changes in marine processes. Nevertheless, it is important to note that current applications of some non-traditional isotopes as paleoceanographic proxies remain a few limits or exist some problems since some processes may affect the isotope records preserved in Fe–Mn crusts and nodules. For instance, postdepositional processes of Fe–Mn (oxyhydr)oxide phases and crust/nodule–seawater interactions, changes in the relative fluxes of metal sources and sinks in the ocean, fractionation processes during metal incorporation at the Fe–Mn crust/nodule surface and metal distribution among Fe–Mn mineral phases. In addition, there is also a great need for a community effort to exploit and enhance in studies on non-traditional isotope geochemistry of marine Fe–Mn crusts and nodules. (1) The precision and accuracy of the analytical methods need to be further improved. For example, in chemical purification of Li, Mg, Cd and Tl from Fe–Mn samples, at least two or three sets of anion and cation exchange chromatography are needed, it is time-consuming and it may also cause isotopic fractionation. So we need to create some new concise and effective chemical purification procedures that can be used to extract the target element. In addition, effective methods for correction of isotope discrimination effects needs further development to avoid isotopic fractionation during MC-ICP-MS measurements. Besides, there needs to be a number of suitable Fe–Mn curst/nodule reference material to help monitoring the entire experiment procedures. (2) Some isotope international standards are needed for the non-traditional stable isotope geochemistry. For instance, currently, the international standards of Zn, Mo, and Cd isotopes are not readily available, and international standard NIST SRM 976 of Cu isotope has been run out. Although some studies have provided the transformation formulae for different isotope reference materials, it is still very inconvenient for the research and application of these isotopes. (3) Although the distributions and fractionations have been reported for some non-traditional isotopes in Fe–Mn crusts/nodules and seawater, the data remain limited and the mechanisms controlling isotopic fractionation for some metals have yet to be clearly explained, particularly for Li, Mg, Cd and Ni isotopes. Therefore it is necessary to investigate more Fe–Mn curst/nodule samples from different ocean areas, and accumulate adequate isotopic data from different reservoirs and different types of natural samples, and further elucidate the factors that control the isotopic fractionation of metals. (4) For many of these promising isotope systems, the molecular scale controls on their isotopic fractionations are needed to be further explored. Different molecular bonding mechanisms of metals to different Fe–Mn crust and

nodule mineral phases (e.g., birnessite, vemadite, todorokite, goethite and ferrihydrite), determined using for example XANES and EXAFS synchrotron radiation data, which may explain the sequence of enrichment and fractionation of metals in marine Fe–Mn deposits. So far, only Cu, Zn Mo and Tl isotopes were carried out some experiments, and there are many extend work to do. (5) Constraining some specific questions using multiple isotopic proxies should be enhanced. For instance, in paleo-redox studies, a particularly promising approach is to combine different isotope systems, taking advantage of their differing redox response, and avoiding the weaknesses associated with the use of a single redox proxy. However, from the previous researches of non-traditional isotopes in Fe–Mn deposits, we can see most of the studies using a single isotope proxy to understand important issues such as paleo-oceanic redox conditions, metal sources, past changes in climatic conditions, even if using the same samples for example CD29-2. (6) Much effort will be applied to develop new non-traditional isotopic proxies in Fe–Mn crusts that reflect the evolution of Cenozoic oceans, atmosphere, and continents. A handful of oceanographically interesting elements such as V, Cr, Te, U and W in Fe–Mn nodules and crusts should be received increasing attention.

Acknowledgements The author greatly thank referees for their careful review of this manuscript and their helpful comments and suggestions.

Funding This work was supported by the National Nature Science Foundation of China (Nos. 41173020 and 41376080).

Availability of data and material The datasets supporting the conclusions of this article are included within the article.

Compliance with ethical standards

Conflict of interest The authors declare that they have no competing interest.

References

Albarède F (2004) The stable isotope geochemistry of Copper and Zinc. Rev Mineral Geochem 55:409–427

Albarède F, Beard B (2004) Analytical methods for non-traditional isotopes. Rev Mineral Geochem 55:113–152

Anbar AD (2004) Molybdenum stable isotopes: observations, interpretations and directions. Rev Mineral Geochem 55:429–454

Anbar AD, Rouxel O (2007) Metal stable isotopes in paleoceanography. Annu Rev Earth Planet Sci 35(1):717–746

Baker RGA, Rehkämper M, Hinkley TK, Nielsen SG, Toutain JP (2009) Investigation of thallium fluxes from subaerial volcanism-Implications for the present and past mass balance of thallium in the oceans. Geochim Cosmochim Acta 73:6340–6359

Banakar VK, Hein JR (2000) Growth response of a deep-water ferromanganese crust to evolution of the Neogene Indian Ocean. Mar Geol 162:529–540

Barling J, Anbar AD (2004) Molybdenum isotope fractionation during adsorption by manganese oxides. Earth Planet Sci Lett 217:315–329

Barling J, Arnold JL, Anbar AD (2001) Natural mass dependent variations in the isotopic composition of molybdenum. Earth Planet Sci Lett 193:447–457

Batley GE, Florence TM (1975) Determination of thallium in natural waters by anodic stripping voltametry. Electroanal Chem Interface Electrochem 61:205–211

Beard BL, Johnson CM (2004) Fe isotope variations in the modern and ancient earth and other planetary bodies. Rev Mineral Geochem 55:319–357

Beard BL, Johnson CM, Von Damm KL, Poulson RL (2003) Iron isotope constraints on Fe cycling and mass balance in oxygenated Earth oceans. Geology 31:629–632

Bermin J, Vance D, Archer C, Statham PJ (2006) The determination of the isotopic composition of Cu and Zn in seawater. Chem Geol 226:280–297

Berner BA (2004) A model for calcium, magnesium and sulfate in seawater over Phanerozoic time. Am J Sci 304:438–453

Berner EK, Berner BA (1987) The global water cycle: geochemistry and environment. Prentice-Hall, Englewood Cliffs, p 80

Bewers JM, Yeats PA (1977) Oceanic residence times of trace-metals. Nature 268(5621):595–598

Bruland KW (1989) Complexation of zinc by natural organic ligands in the Central North Pacific. Limnol Oceanogr 34(2):269–285

Bruland KW, Lohan MC (2003) Controls of trace metals in seawater. Treatise Geochem 6:23–47

Bryan AL, Dong S, Wilkes EB, Wasylenki LE (2015) Zinc isotope fractionation during adsorption onto Mn oxyhydroxide at low and high ionic strength. Geochim Cosmochim Acta 157:182–197

Burton KW, Bourdon B, Birck JL (1999) Osmium isotope variations in the oceans recorded by Fe–Mn crusts. Earth Planet Sci Lett 171:185–197

Cameron V, Vance D (2014) Heavy nickel isotope compositions in rivers and the oceans. Geochim Cosmochim Acta 128:195–211

Cameron V, Vance D, Archer C, House CH (2009) A biomarker based on the stable isotopes of nickel. Proc Natl Acad Sci USA 106:10944–10948

Chan LH, Edmond JM (1988) Variation of lithium isotope composition in the marine environment: a preliminary report. Geochim Cosmochim Acta 52:1711–1717

Chan LH, Hein JR (2007) Lithium contents and isotopic compositions of ferromanganese deposits from the global ocean. Deep-Sea Res II 54(11–13):1147–1162

Chen TY, Ling HF, Hu R, Frank M, Jiang SY (2013) Lead isotope provinciality of central North Pacific Deep Water over the Cenozoic. Geochem Geophys Geosyst 14:1523–1537

Chever F, Rouxel OJ, Croot PL, Ponzevera E, Wuttig K, Auro M (2015) Total dissolvable and dissolved iron isotopes in the water column of the Peru upwelling regime. Geochim Cosmochim Acta 162(1):66–82

Christensen JN, Halliday AN, Godfrey LV (1997) Climate and ocean dynamics and the lead isotopic records in Pacific ferromanganese crusts. Science 277:913–918

Chu N-C, Johnson CM, Beard BL, German CR, Nesbitta RW, Frank M, Marcel B, Kubik PW, Usui A, Graham I (2006) Evidence for hydrothermal venting in Fe isotope compositions of the deep Pacific Ocean through time. Earth Planet Sci Lett 245:202–217

Coale KH, Bruland KW (1988) Copper complexation in the Northeast Pacific. Limnol Oceanogr 33(5):1084–1101

Coale KH, Bruland KW (1990) Spatial and temporal variability in copper complexation in the North Pacific. Deep Sea Research Part A. Oceanogr Res Papers 37(2):317–336

Collier RW (1985) Molybdenum in the northeast Pacific Ocean. Limnol Oceanogr 30:1351–1354

Collier RW, Edmond JM (1984) The trace element geochemistry of marine biogenic particulate matter. Prog Oceanogr 13(2):113–199

Conrad T, Hein JR, Paytan A, Clague DA (2017) Formation of Fe–Mn crusts within a continental margin environment. Ore Geol Rev 87:25–40

Conway TM, John SG (2014) The biogeochemical cycling of zinc and zinc isotopes in the North Atlantic Ocean. Global Biogeochem Cycles 28:1111–1128

Conway TM, John SG (2015) The cycling of iron, zinc and cadmium in the North East Pacific Ocean—insights from stable isotopes. Geochim Cosmochim Acta 164:262–283

Dahl TW, Chappaz C, Fitts JP, Lyons TW (2013) Molybdenum reduction in a sulfidic lake: evidence from X-ray absorption fine-structure spectroscopy and implications for the Mo paleoproxy. Geochim Cosmochim Acta 103(15):213–231

Dauphas N, Pourmand A, Teng FZ (2009) Routine isotopic analysis of iron by HR-MC-ICPMS: how precise and how accurate? Chem Geol 267(3–4):175–184

de Villiers S, Dickson JAD, Ellam RM (2005) The composition of the continental river weathering flux deduced from seawater Mg isotopes. Chem Geol 216:133–142

Edmond JM, Measures C, McDuff RE, Chan LH, Collier R, Grant B, Gordon LI, Corliss JB (1979) Ridge crest hydrothermal activity and the balances of the major and minor elements in the ocean: the Galapagos data. Earth Planet Sci Lett 46:1–18

Elderfield H, Schultz A (1996) Mid-ocean ridge hydrothermal fluxes and the chemical composition of the ocean. Annu Rev Earth Planet Sci 24:191–224

Erickson BE, Helz GR (2000) Molybdenum (VI) speciation in sulfidic waters: stability and lability of thiomolybdates. Geochim Cosmochim Acta 64(7):1149–1158

Firdaus LM, Norisuye K, Nakagawa Y, Nakatsuka S, Sohrin Y (2008) Dissolved and labile particulate Zr, Hf, Nb, Ta, Mo and W in the western North Pacific Ocean. J Oceanogr 64:247–257

Fitzsimmons JN, Carrasco GG, Wu J, Roshan M, Hatta M, Measures CI, Conway TM, John SG, Boyle EA (2015) Partitioning of dissolved iron and iron isotopes into soluble and colloidal phases along the U.S. GEOTRACES North Atlantic Transect. Deep Sea Res Part II 116:130–151

Flegal AR, Patterson CC (1985) Thallium concentrations in seawater. Mar Chem 15(4):327–331

Frank M (2002) Radiogenic isotopes: tracers of past ocean circulation and erosional input. Rev Geophys 40(1):1–38

Frank M, O'Nions RK, Hein JR, Banakar VK (1999) 60 Myr records of major elements and Pb-Nd isotopes from hydrogenous ferromanganese crusts: reconstruction of seawater paleochemistry. Geochim Cosmochim Acta 63:1689–1708

Frew R, Bowie A, Croot P, Pickmere S (2001) Macronutrient and trace-metal geochemistry of an in situ iron-induced Southern Ocean bloom. Deep-Sea Res II 48:2467–2481

Fu YZ, Wang ZR (2012) Mg isotope variation in a ferromanganese crust from Line Seamount in the Central Pacific Ocean. Mineral Mag 76(6):1722

Fu YZ, Peng JT, Qu WJ, Hu RZ, Shi XF, Du AD (2005) Os isotopic compositions of a cobalt-rich ferromanganese crust profile in Central Pacific. Chin Sci Bull 50(18):2106–2112

Gaillardet J, Viers J, Dupre B (2003) Trace elements in river waters. Treatise Geochem Surf Ground Water Weather Soils 5:225–272

Gall L, Williams HM, Siebert C (2013) Nickel isotopic compositions of ferromanganese crusts and the constancy of deep ocean inputs and continental weathering effects over the Cenozoic. Earth Planet Sci Lett 375:148–155

Galy A, Belshaw NS, Halicz L, O'Nions RK (2001) High-precision measurement of magnesium isotopes by multiple-collector inductively coupled plasma mass spectrometry. Int J Mass Spectrom 208(1–3):89–98

Galy A, Yoffe O, Janney PE, Williams RW, Cloquet C, Alard O, Halicz L, Wadhwa M, Hutcheon ID, Ramon E, Carignan J (2003) Magnesium isotope heterogeneity of the isotopic standard SRM980 and new reference materials for magnesium-isotope-ratio measurements. J Anal Spectrom 18:1352–1356

Goldberg T, Archer C, Vance D, Poulton SW (2009) Mo isotope fractionation during adsorption to Fe (oxyhydr) oxides. Geochim Cosmochim Acta 73:6502–6516

Goto KT, Shimoda G, Anbar AD, Gordon GW, Harigane Y, Senda R, Suzuki K (2015) Molybdenum isotopes in hydrothermal manganese crust from the Ryukyu arc system: implications for the source of molybdenum. Mar Geol 369:91–99

Gramlish J, Machlan L, Barnes I, Paulsen P (1989) Absolute isotopic abundance ratios and atomic weight of a reference sample of nickel. J Res Natl Inst Stand Tech 94:347–356

Gueguen B, Rouxel O, Rouget ML, Bollinger C, Ponzevera E, Germain Y, Fouquet Y (2016) Comparative geochemistry of four ferromanganese crusts from the Pacific Ocean and significance for the use of Ni isotopes as paleoceanographic tracers. Geochim Cosmochim Acta 189:214–235

Halliday AN, Lee DC, Christensen JN, Walder AJ, Freedman PA, Jones CE, Hall CM, Yi W, Teagle D (1995) Recent developments in inductively coupled plasma magnetic sector multiple collector mass spectrometry. Int J Mass Spectrom Ion Processes 146–147(31):21–33

Hein JR (2004) Cobalt-rich ferromanganese crusts: Global distribution, composition, origin, and research activities, minerals other than polymetallic nodules of the international seabed area, chapter: 5. International Seabed Authority, Kingston, pp 188–256

Hein JR, Koschinsky A (2014) Deep-ocean ferromanganese crusts and nodules. In: Holland HD, Turekian KK (eds) Treatise on Geochemistry, 2nd edn, volume 13, chapter 11. Elsevier, Amsterdam, pp 273–291

Hein JR, Koschinsky A, Bau M, Manheim FT, Kang JK, Roberts L (2000) Cobalt-rich ferromanganese crusts in the Pacific. In: Cronan DS (ed) Handbook of marine mineral deposits. CRC Press, Boca Raton, pp 239–279

Hein JR, Mizell K, Koschinsky A, Conrad TA (2013) Deep-ocean mineral deposits as a source of critical metals for high- and green technology applications: comparison with land-based resources. Ore Geol Rev 51:1–14

Hoefs J (2015) Stable isotope geochemistry, 7th edn. Springer International Publishing, Berlin

Horner TJ, Schönbächler M, Rehkämper M, Nielsen SG, Williams H, Halliday AN, Xue Z, Hein JR (2010) Ferromanganese crusts as archives of deep water Cd isotope compositions. Geochem Geophys Geosyst 11(4):1–10

Horner TJ, Williams HM, Hein JR, Saito MA, Burton KW, Halliday AN, Nielsen SG (2015) Persistence of deeply sourced iron in the Pacific Ocean. PNAS 112:1292–1297

Huh Y, Chan LH, Zhang L, Edmond JM (1998) Lithium and its isotopes in major world rivers: implications for weathering and the oceanic budget. Geochim Cosmochim Acta 62:2039–2051

Huh Y, Chan LH, Edmond JM (2001) Lithium isotopes as a probe of weathering processes: Orinoco River. Earth Planet Sci Lett 194:189–199

Jiang SY, Jon W, Yu JM, Pan JY, Liao QL, Wu NP (2000) A reconnaissance of Cu isotope composition of hydrothermal copper deposit, Jinman, Yunnan, China. Chin Sci Bull 47(3):247–250

Johnson KS, Gordon RM, Coale KH (1997) What controls dissolved iron concentrations in the world ocean? Mar Chem 57:137–161

Juillot F, Marechal C, Ponthieu M (2008) Zn isotopic fractionation caused by sorption on goethite and 2-lines ferrihydrite. Geochim Cosmochim Acta 72:4886–4900

Kashiwabara T, Takahashi Y, Tanimizu M, Usui A (2011) Molecular-scale mechanisms of distribution and isotopic fractionation of molybdenum between seawater and ferromanganese oxides. Geochim Cosmochim Acta 75(19):5762–5784

Klemm V, Levasseur S, Frank M, Hein JR, Halliday AN (2005) Osmium isotope stratigraphy of a marine ferromanganese crust. Earth Planet Sci Lett 238:42–48

Kurzweil F, Wille M, Schoenberg R, Taubald H, Van Kranendonk MJ (2015) Continuously increasing δ^{98}Mo values in Neoarchean black shales and iron formations from the Hamersley Basin. Geochim Cosmochim Acta 164:523–542

Lacan F, Francois R, Ji YC, Sherrell RM (2006) Cadmium isotopic composition in the ocean. Geochim Cosmochim Acta 70(20):5104–5118

Lee DC, Halliday AN, Hein JR, Burton KW, Christensen JN, Gunther D (1999) Hafnium isotope stratigraphy of ferromanganese crusts. Science 285:1052–1054

Levasseur S, Frank M, Hein JR (2004) The global variation in the iron isotope composition of marine hydrogenetic ferromanganese deposits: implications for seawater chemistry? Earth Planet Sci Lett 224(1/2):91–105

Li H-Y, Schoonmaker J (2003) Chemical composition and mineralogy of marine sediments. Treatise Geochem Sediments Diagenesis Sediment Rocks 7:1–35

Ling HF, Burton KW, Onions RK, Kamber BS, von Blanckenburg F, Gibb AJ, Hein JR (1997) Evolution of Nd and Pb isotopes in Central Pacific seawater from ferromanganese crusts. Earth Planet Sci Lett 146(1–2):1–12

Ling HF, Jiang SY, Frank M, Zhou HY, Zhou F, Lu ZL, Chen XM, Jiang YH, Ge CD (2005) Differing controls over the Cenozoic Pb and Nd isotope evolution of deepwater in the central North Pacific Ocean. Earth Planet Sci Lett 232(3–4):345–361

Little SH, Vance D, Walker-Brown C, Landing WM (2014a) The oceanic mass balance of copper and zinc isotopes, investigated by analysis of their inputs and oxic outputs in ferromanganese crusts. Geochim Cosmochim Acta 125:673–693

Little SH, Sherman DM, Vance D (2014b) Molecular controls on Cu and Zn isotopic fractionation in Fe–Mn crusts. Earth Planet Sci Lett 396:213–222

Little SH, Vance D, Lyons TW, McManus J (2015) Controls on trace metal authigenic enrichment in reducing sediments: insights from modern oxygen-deficient settings. Am J Sci 315:77–119

Little SH, Vance D, McManus J, Severmann S (2016) Critical role of continental margin sediments in the oceanic mass balance of Zn and Zn isotopes. Geology 44:207–210

Mackey D, O'Sullivan J, Watson R, DalPont G (2002) Trace metals in the Western Pacific: temporal and spatial variability in the concentrations of Cd, Cu, Mn and Ni. Deep-Sea Res I 49:2241–2259

Marcus MA, Edwards KJ, Gueguen B, Fakra SC, Horn G, Jelinski NA, Rouxel O, Sorensen J, Toner BM (2015) Iron mineral structure, reactivity, isotopic composition in a South Pacific Gyre ferromanganese nodule over 4 Ma. Geochim Cosmochim Acta 171:61–79

Maréchal CN, Albarède F (2002) Ion-exchange fractionation of copper and zinc isotopes. Geochim Cosmochim Acta 66(9):1499–1509

Maréchal CN, Télouk P, Albarède F (1999) Precise analysis of copper and zinc isotopic compositions by plasma-source mass spectrometry. Chem Geol 156(1–4):251–273

Maréchal CN, Nicolas E, Douchet C, Albarède F (2000) Abundance of zinc isotopes as a marine biogeochemical tracer. Geochem Geophys Geosyst 1(1):1–15

Mathur R, Ruiz J, Titley S, Liermann L, Buss H, Brantley S (2005) Cu isotopic fractionation in the supergene environment with and without bacteria. Geochim Cosmochim Acta 69(22):5233–5246

MBARI (2012) Monterey Bay Aquarium Research Institute: periodic table of elements in the ocean. http://www.mbari.org/chemsensor/pteo.htm

McDonough WF, Sun S-S (1995) The composition of the Earth. Chem Geol 120(3–4):223–253

McManus J, Nägler TF, Siebert C, Wheat CG, Hammond DE (2002) Oceanic molybdenum isotope fractionation: diagenesis and hydrothermal ridge-flank alteration. Geochem Geophys Geosyst 3(12):1–9

McMurtry GM, VonderHaar DL, Eisenhauer A, Mahoney JJ, Yeh HW (1994) Cenozoic accumulation history of a Pacific ferromanganese crust. Earth Planet Sci Lett 125:105–118

Miller CA, Peucker-Ehrenbrink B, Walker BD, Marcantonio F (2011) Re-assessing the surface cycling of molybdenum and rhenium. Geochim Cosmochim Acta 75:7146–7179

Millet MA, Baker JA, Payne CE (2012) Ultra-precise stable Fe isotope measurements by high resolution multiple-collector inductively coupled plasma mass spectrometry with a ^{57}Fe–^{58}Fe double-spike. Chem Geol 304:18–25

Millot R, Guerrot C, Vigier N (2004) Accurate and high precision measurement of lithium isotopes in two reference materials by MC-ICP-MS. Geostand Geoanal Res 28:153–159

Misra S, Froelich PN (2009) Measurement of lithium isotope ratios by quadrupole-ICP-MS: application to seawater and natural carbonates. J Anal At Spectrom 24(11):1524–1533

Misra S, Froelich PN (2012) Lithium isotope history of Cenozoic seawater: changes in silicate weathering and reverse weathering. Science 335:818–823

Nielsen SG, Rehkämper M, Baker J, Halliday AN (2004) The precise and accurate determination of thallium isotope compositions and concentrations for water samples by MC-ICPMS. Chem Geol 204(1–2):109–124

Nielsen SG, Rehkämper M, Teagle DAH, Butterfield DA, Alt JC, Halliday AN (2006) Hydrothermal fluid fluxes calculated from the isotopic mass balance of thallium in the ocean crust. Earth Planet Sci Lett 251:120–133

Nielsen SG, Mar-Gerrison S, Gannoun A, LaRowe D, Klemm V, Halliday AN, Burton KW, Hein JR (2009) Thallium isotope evidence for a permanent increase in marine organic carbon export in the early Eocene. Earth Planet Sci Lett 278:297–307

Nielsen SG, Gannoun A, Marnham C, Burton KW, Halliday AN, Hein JR (2011) New age for ferromanganese crust 109D-C and implications for isotopic records of lead, neodymium, hafnium, and thallium in the Pliocene Indian Ocean. Paleoceanography 26:1–23

Nielsen SG, Wasylenki LE, Rehkämper M (2013) Towards an understanding of thallium isotope fractionation during adsorption to manganese oxides. Geochim Cosmochim Acta 117:252–265

O'Nions RK, Frank M, von Blanckenburg F, Ling HF (1998) Secular variation of Nd and Pb isotopes in ferromanganese crusts from the Atlantic, Indian and Pacific Oceans. Earth Planet Sci Lett 155:15–28

Owens JD, Nielsen SG, Horner TJ (2017) Thallium-isotopic compositions of euxinic sediments as a proxy for global manganese-oxide burial. Geochim Cosmochim Acta 213:291–307

Peacock CL, Moon EM (2012) Oxidative scavenging of thallium by birnessite: explanation for thallium enrichment and stable isotope fractionation in marine ferromanganese precipitates. Geochim Cosmochim Acta 84:297–313

Peucker-Ehrenbrink B, Ravizza G, Hofmann AW (1995) The marine ^{187}Os/^{186}Os record of the past 80 million years. Earth Planet Sci Let 130:155–167

Ponthieu M, Juillot F, Hiemstra T, van Riemsdijk WH, Benedetti MF (2006) Metal ion binding to iron oxides. Geochim Cosmochim Acta 70:2679–2698

Radic A, Lacan F, Murray JW (2011) Iron isotopes in the seawater of the equatorial Pacific Ocean: new constraints for the oceanic iron cycle. Earth Planet Sci Lett 306:1–10

Rehkämper M, Halliday AN (1999) The precise measurement of Tl isotopic compositions by MC-ICPMS: application to the analysis of geological materials and meteorites. Geochim Cosmochim Acta 63(6):935–944

Rehkämper M, Nielsen SG (2004) The mass balance of dissolved thallium in the oceans. Mar Chem 85:125–139

Rehkämper M, Frank M, Hein JR, Porcelli D, Halliday AN, Ingri J, Liebetrau V (2002) Thallium isotope variation sin seawater and hydrogenetic, diagenetic, and hydrothermal ferromanganese deposits. Earth Planet Sci Let 197:65–81

Rehkämper M, Frank M, Hein JR, Halliday AN (2004) Cenozoic marine geochemistry of thallium deduced from isotopic studies of ferromanganese crusts and pelagic sediments. Earth Planet Sci Lett 219:77–91

Riley JP, Tongudai M (1964) The lithium content of sea water. Deep-sea Res Oceanogr Abstr 11:563–568

Ripperger S, Rehkämper M (2007) Precise determination of cadmium isotope fractionation in seawater by double-spike MC-ICPMS. Geochim Cosmochim Acta 71:631–642

Ripperger S, Rehkämper M, Porcelli D, Halliday AN (2007) Cadmium isotope fractionation in seawater: a signature of biological activity. Earth Planet Sci Lett 261(3–4):670–684

Rose-Koga E, Albarede FA (2010) Data brief on magnesium isotope compositions of marine calcareous sediments and ferromanganese nodules. Geochem Geophys Geosyst 11(3):1–12

Rosenthal Y, Lam P, Boyle EA, Thomson J (1995) Authigenic cadmium enrichments in suboxic sediments: precipitation and post depositional mobility. Earth Planet Sci Lett 132(1–4):99–111

Saager PM, de Baar HJW, Howland RJ (1992) Cd, Zn, Ni and Cu in the Indian Ocean. Deep-Sea Res 39:9–35

Saager PM, de Baar HJW, de Jong JTM, Nolting RF, Schijf J (1997) Hydrography and local sources of dissolved trace metals Mn, Ni, Cu and Cd in the northeast Atlantic Ocean. Mar Chem 57:195–216

Schauble EA (2004) Applying stable isotope fractionation theory to new systems. In: Johnson CM, Beard BL, Albarede F (eds) Geochemistry of non-traditional stable isotopes, reviews in mineralogy and geochemistry, vol 55. Mineralogical Society of America, Geochemical Society

Schmitt AD, Galer SJG, Abouchami W (2009) Mass-dependent cadmium isotopic variations in nature with emphasis on the marine environment. Earth Planet Sci Lett 277(1–2):262–272

Sclater F, Boyle E, Edmond J (1976) On the marine geochemistry of nickel. Earth Planet Sci Lett 31:119–128

Shields WR, Murphy TJ, Garner EL (1964) Absolute isotopic abundance ratio and the atomic weight of a reference sample of copper. J Res NBS 68A:589–592

Siebert C, Nagler TF, von Blanckenburg F, Kramers JD (2003) Molybdenum isotope records as a potential new proxy for paleoceanography. Earth Planet Sci Lett 211:159–171

Siebert J, Corgne A, Ryerson FJ (2011) Systematics of metal–silicate partitioning for many siderophile elements applied to Earth's core formation. Geochim Cosmochim Acta 75:1451–1489

Simpson WR (1978) A critical review of Cadmium in the Marine environment. Prog Oceanogr 10(1):1–70

Sinoir M, Butler ECV, Bowie AR, Mongin M, Nesterenko PN, Hassler CS (2012) Zinc marine biogeochemistry in seawater: a review. Mar Freshwater Res 63:644–657

Takano S, Tanimizu M, Hirata T, Sohrin Y (2014) Isotopic constraints on biogeochemical cycling of copper in the ocean. Nat Commun 5:5663. https://doi.org/10.1038/ncomms6663

Taylor SR, McLennan SM (1985) The continental crust: its composition and evolution. An examination of the geochemical record preserved in sedimentary rocks. Blackwell Scientific Publishing, Oxford

Teng FZ, Wadhwa M, Helz RT (2007) Investigation of magnesium isotope fractionation during basalt differentiation: implications for a chondritic composition of the terrestrial mantle. Earth Planet Sci Lett 261:84–92

Teng FZ, Dauphas N, Watkins JM (2017) Non-traditional stable isotopes: retrospective and prospective. Rev Mineral Geochem 82:1–26

Thompson CM, Ellwood MJ, Sander SG (2014) Dissolved copper speciation in the Tasman Sea, SW Pacific Ocean. Mar Chem 164:84–94

Tipper ET, Galy A, Gaillardet J, Bickle MJ, Elderfield H, Carder EA (2006) The magnesium isotope budget of the modern ocean: constraints from riverine magnesium isotope ratios. Earth Planet Sci Lett 250:241–253

Tomascak PB (2004) Developments in the understanding and application of lithium isotopes in the earth and planetary sciences. Rev Mineral Geochem 55:153–195

Usui A, Nishi K, Satoa H, Nakasato Y, Thornton B, Kashiwabara T, Tokumaru A, Sakaguchi A, Yamaoka K, Kato S, Nitahara S, Suzuki K, Lijima K, Urabe T (2017) Continuous growth of hydrogenetic ferromanganese crusts since 17 Myr ago on Takuyo-Daigo Seamount, NW Pacific, at water depths of 800–5500 m. Ore Geol Rev 87:71–87

Vance D, Archer C, Bermin J, Perkins J, Statham PJ, Lohan MC, Ellwood MJ, Mills RA (2008) The copper isotope geochemistry of rivers and the oceans. Earth Planet Sci Lett 274(1–2):204–213

Wasylenki LE, Weeks CL, Bargar JR, Spiro TG, Hein JR, Anbar AD (2011) The molecular mechanism of Mo isotope fractionation during adsorption to birnessite. Geochim Cosmochim Acta 75(17):5019–5031

Wieser ME, De Laeter JR, Varner MD (2007) Isotope fractionation studies of molybdenum. Internat J Mass Spec 265:40–48

Wilkinson BG, Algeo TJ (1989) Sedimentary carbonate record of calcium-magnesium cycling. Am J Sci 289(10):1158–1194

Xue ZC, Rehkämper M, Horner TJ, Abouchami W, Middag R, van de Flierdt T, de Baar HJW (2013) Cadmium isotope variations in the Southern Ocean. Earth Planet Sci Lett 382:161–172

Young ED, Galy A (2004) The isotope geochemistry and cosmochemistry of magnesium. Rev Mineral Geochem 55:197–230

Zhao Y, Vance D, Abouchami W, de Baar HJW (2014) Biogeochemical cycling of zinc and its isotopes in the Southern Ocean. Geochim Cosmochim Acta 125:653–672

Zhu XK, O'Nions RK, Guo YL, Reynolds BC (2000) Secular variation of iron isotopes in north Atlantic deep water. Science 287:2000–2002

Zhu XK, Guo Y, O'Nions RK, Young ED, Ash RD (2001) Isotopic homogeneity of iron in the early solar nebula. Nature 412:311–313